

Microwave conductivity due to impurity scattering in cuprate superconductors

Minghuan Zeng, Xiang Li, Yongjun Wang, and Shiping Feng*
Department of Physics, Beijing Normal University, Beijing 100875, China

The microwave surface impedance measurements on cuprate superconductors provide the crucial information of the effect of the impurity scattering on the quasiparticle transport, however, the full understanding of the effect of the impurity scattering on the quasiparticle transport is still a challenging issue. Here based on the microscopic octet scattering model, the effect of the impurity scattering on the low-temperature microwave conductivity in cuprate superconductors is investigated in the self-consistent T -matrix approach. The impurity-dressed electron propagator obtained in the Fermi-arc-tip approximation of the quasiparticle excitations and scattering processes is employed to derive the electron current-current correlation function by taking into account the impurity-induced vertex correction. It is shown that the microwave conductivity spectrum is a non-Drude-like, with a sharp cusp-like peak extending to zero-energy and a high-energy tail falling slowly with energy. Moreover, the microwave conductivity decreases with the increase of the impurity concentration or with the increase of the strength of the impurity scattering potential. In a striking contrast to the dome-like shape of the doping dependence of the superconducting transition temperature, the microwave conductivity exhibits a reverse dome-like shape of the doping dependence. The theory also show that the highly unconventional features of the microwave conductivity are generated by both the strong electron correlation and impurity-scattering effects.

PACS numbers: 74.25.Nf, 74.62.Dh, 74.25.Fy, 74.72.-h

I. INTRODUCTION

For a conventional superconductor with a s-wave pairing symmetry, the impurity scattering has little effect on superconductivity^{1,2}. However, cuprate superconductors are anomalously sensitive to the impurity scattering³⁻⁶, since superconductivity involves a pairing state with the dominant d-wave symmetry⁷. In particular, the superconducting (SC) transition temperature T_c in cuprate superconductors is systematically diminished with impurities⁸⁻¹⁵, which therefore confirms definitely that the impurity scattering has high impacts on superconductivity³⁻⁶. In this case, the understanding of the effect of the impurity scattering on superconductivity is a central issue for cuprate superconductors.

Among the striking features of the SC-state in cuprate superconductivity, the physical quantity which most evidently displays the dramatic effect of the impurity scattering on superconductivity is the quasiparticle transport³⁻⁶, which is manifested by the microwave conductivity. This microwave conductivity contains a wealth of the information on the SC-state quasiparticle response, and is closely associated with the superfluid density³⁻⁶. By virtue of systematic studies using the microwave surface impedance measurements, the low-temperature features of the SC-state quasiparticle transport in cuprate superconductors have been well established^{3-6,16-20}, where an agreement has emerged that the microwave conductivity are dominated mainly by thermally excited quasiparticles being scattered by impurities. In particular, as an evidence of the very long-live quasiparticle excitation deep in the SC-state, the low-temperature microwave conductivity spectrum has a cusp-like shape of the energy dependence¹⁶⁻²⁰. However, it is still unclear how this microwave conduc-

tivity evolves with the impurity concentration. Moreover, the experimental observations have also shown that even minor concentrations of impurities lead to changes in the temperature dependence of the magnetic-field penetration-depth from linear in the pure systems to quadratic²¹, while the ratio of the low-temperature superfluid density and effective mass of the electrons $n_s(T \rightarrow 0)/m^*$ is decreased when one increases the impurity concentration²²⁻²⁴.

In the d-wave SC-state of cuprate superconductors, the SC gap vanishes along the nodal direction of the electron Fermi surface (EFS)⁷, and then as a natural consequence, the most properties well below T_c ought to be controlled by the quasiparticle excitations at around the nodal region of EFS. In this case, the d-wave Bardeen-Cooper-Schrieffer (BCS) type formalism³⁻⁶, incorporating the effect of the impurity scattering within the self-consistent T -matrix approach, has been employed to study the effect of the impurity scattering on the microwave conductivity of cuprate superconductors²⁵⁻³², where the impurity scattering self-energy was evaluated in the nodal approximation of the quasiparticle excitations and scattering processes, and then was used to calculate the electron current-current correlation function by including the contributions of the impurity-induced vertex correction and Fermi-liquid correction²⁶⁻³¹. The obtained results show that both the impurity-induced vertex correction and Fermi-liquid correction modify the microwave conductivity²⁶⁻³¹. However, (i) although the contribution from the Fermi-liquid correction is included, these treatments suffer from ignoring the strong electron correlation effect in the homogenous part of the electron propagator²⁵⁻³¹, while this strong electron correlation effect also plays an important role in the SC-state quasiparticle transport; (ii) moreover, the angle-resolved pho-

to emission spectroscopy (ARPES) experiments^{33–35} have shown clearly that the Fermi arcs that emerge due to the EFS reconstruction at the case of zero energy^{36–43} can persist into the case for a finite binding-energy, where a particularly large fraction of the spectral weight is located at around the tips of the Fermi arcs. These tips of the Fermi arcs connected by the scattering wave vectors \mathbf{q}_i thus construct an *octet scattering model*, and then the quasiparticle scattering with the scattering wave vectors \mathbf{q}_i contribute effectively to the quasiparticle scattering processes^{33–35}. In particular, this octet scattering model has been employed to give a consistent explanation of the experimental data detected from Fourier transform scanning tunneling spectroscopy^{44–48} and the ARPES autocorrelation pattern observed from ARPES experiments^{33–35}. These experimental results^{33–48} therefore have shown clearly that the shape of EFS has deep consequences for the various properties of cuprate superconductors, while such an aspect should be also reflected in the SC-state quasiparticle transport.

In the recent work⁴⁹, we have started from the homogenous part of the electron propagator and the related *microscopic octet scattering model*, which are obtained within the framework of the kinetic-energy-driven superconductivity^{50–53}, to discuss the influence of the impurity scattering on the electronic structure of cuprate superconductors in the self-consistent T -matrix approach, where the impurity scattering self-energy is derived in the *Fermi-arc-tip approximation* of the quasiparticle excitations and scattering processes, and then the impurity-dressed electron propagator incorporates both the strong electron correlation effect and the impurity-scattering effect. The obtained results⁴⁹ show that the decisive role played by the impurity scattering self-energy in the particle-hole channel is the further renormalization of the quasiparticle band structure with a reduced quasiparticle lifetime, while the impurity scattering self-energy in the particle-particle channel induces a strong deviation from the d-wave behaviour of the SC gap, leading to the existence of a finite gap over the entire EFS. In this paper, we study the effect of the impurity scattering on the microwave conductivity in cuprate superconductors along with this line by taking into account the impurity-induced vertex correction, where the impurity-dressed electron propagator⁴⁹ is employed to evaluate the vertex-corrected electron current-current correlation function in the self-consistent T -matrix approach, and the obtained results in the Fermi-arc-tip approximation of the quasiparticle excitations and scattering processes show that the low-temperature microwave conductivity spectrum is a non-Drude-like, with a sharp cusp-like peak extending to zero-energy and a high-energy tail falling slowly with energy, in agreement with the corresponding experiments^{16–20}. In particular, although the low-energy cusp-like peak decay as $\rightarrow 1/[\omega + \text{constant}]$, the overall shape of the microwave conductivity spectrum exhibits a special non-Drude-like behavior with the depicted formula that has been also used to fit the corresponding

experimental data in Ref. 19. Moreover, the microwave conductivity decreases with ascending impurity concentration or with rising strength of the impurity scattering potential. Our these results therefore show that the highly unconventional features of the microwave conductivity are induced by both the strong electron correlation and impurity-scattering effects.

The remainder of this paper is organized as follows: Sec. II contains details regarding the calculation technique of the microwave conductivity in the presence of the impurity scattering. The quantitative characteristics of the impurity-scattering effect on the doping and energy dependence of the microwave conductivity are presented in Sec. III, where we show that in a striking contrast to the dome-like shape doping dependence of T_c , the minimum of the microwave conductivity occurs at around the optimal doping, and then increases in both underdoped and overdoped regimes. Finally, we give a summary in Sec. IV. In the Appendix, we present the details of the derivation of the vertex kernels of the electron current-current correlation function.

II. THEORETICAL FRAMEWORK

It was recognized shortly after the discovery of superconductivity in cuprate superconductors that the essential physics of cuprate superconductors is contained in the square-lattice t - J model^{54,55},

$$H = - \sum_{l'l\sigma} t_{ll'} C_{l\sigma}^\dagger C_{l'\sigma} + \mu \sum_{l\sigma} C_{l\sigma}^\dagger C_{l\sigma} + J \sum_{l\hat{\eta}} \mathbf{S}_l \cdot \mathbf{S}_{l+\hat{\eta}}, \quad (1)$$

where $C_{l\sigma}^\dagger$ ($C_{l\sigma}$) creates (annihilates) a constrained electron with spin index $\sigma = \uparrow, \downarrow$ on lattice site l , \mathbf{S}_l is spin operator with its components S_l^x , S_l^y , and S_l^z , and μ is the chemical potential. The kinetic-energy part includes the electron-hopping term $t_{ll'} = t_{\hat{\eta}} = t$ between the nearest-neighbor (NN) sites $\hat{\eta}$ and the electron-hopping term $t_{ll'} = t_{\hat{\eta}'} = t'$ between the next NN sites $\hat{\eta}'$, while the magnetic-energy part is described by a Heisenberg term with the magnetic interaction J between the NN sites $\hat{\eta}$. As a qualitative discussion, the commonly used parameters in the t - J model (1) are chosen as $t/J = 2.5$ and $t'/t = 0.3$ as in our previous discussions⁴⁹. However, when necessary to compare with the experimental data, we set $J = 1000\text{K}$.

The basis set of the t - J model (1) is restricted by the requirement that no lattice site may be doubly occupied by electrons^{56–59}, i.e., $\sum_{\sigma} C_{l\sigma}^\dagger C_{l\sigma} \leq 1$. Our method employs a fermion-spin theory description of the t - J model (1) together with the on-site local constraint of no double electron occupancy^{52,60}, where the constrained electron operators $C_{l\uparrow}$ and $C_{l\downarrow}$ in the t - J model (1) are separated into two distinct operators as,

$$C_{l\uparrow} = h_{l\uparrow}^\dagger S_l^-, \quad C_{l\downarrow} = h_{l\downarrow}^\dagger S_l^+, \quad (2)$$

with the spinful fermion operator $h_{l\sigma} = e^{-i\Phi_{l\sigma}} h_l$ that describes the charge degree of freedom of the constrained

electron together with some effects of spin configuration rearrangements due to the presence of the doped hole itself (charge carrier), while the spin operator S_l that represents the spin degree of freedom of the constrained electron, and then the local constraint of no double electron occupancy is fulfilled in actual analyses.

Starting from the t - J model (1) in the fermion-spin representation (2), the kinetic-energy-driven SC mechanism has been established^{50–53}, where the charge carriers are held together in the d-wave pairs in the particle-particle channel due to the effective interaction, which originates directly from the kinetic energy of the t - J model (1) in the fermion-spin representation (2) by the exchange of spin excitations, then the d-wave electron pairs originating from the d-wave charge-carrier pairing state are due to the charge-spin recombination, and their condensation reveals the d-wave SC-state. In these previous discussions, the homogenous electron propagator of the t - J model (1) in the SC-state has been obtained explicitly in the Nambu representation as⁵³,

$$\begin{aligned}\tilde{G}(\mathbf{k}, \omega) &= \begin{pmatrix} G(\mathbf{k}, \omega), & \mathfrak{S}(\mathbf{k}, \omega) \\ \mathfrak{S}^\dagger(\mathbf{k}, \omega), & -G(\mathbf{k}, -\omega) \end{pmatrix} \\ &= \frac{1}{F(\mathbf{k}, \omega)} \{ [\omega - \Sigma_0(\mathbf{k}, \omega)]\tau_0 + \Sigma_1(\mathbf{k}, \omega)\tau_1 \\ &\quad + \Sigma_2(\mathbf{k}, \omega)\tau_2 + [\varepsilon_{\mathbf{k}} + \Sigma_3(\mathbf{k}, \omega)]\tau_3 \},\end{aligned}\quad (3)$$

where τ_0 is the unit matrix, τ_1 , τ_2 , and τ_3 are Pauli matrices, $\varepsilon_{\mathbf{k}} = -4t\gamma_{\mathbf{k}} + 4t'\gamma'_{\mathbf{k}} + \mu$ is the energy dispersion in the tight-binding approximation, with $\gamma_{\mathbf{k}} = (\cos k_x + \cos k_y)/2$, $\gamma'_{\mathbf{k}} = \cos k_x \cos k_y$, $F(\mathbf{k}, \omega) = [\omega - \Sigma_0(\mathbf{k}, \omega)]^2 - [\varepsilon_{\mathbf{k}} + \Sigma_3(\mathbf{k}, \omega)]^2 - \Sigma_1^2(\mathbf{k}, \omega) - \Sigma_2^2(\mathbf{k}, \omega)$, and the homogenous self-energy has been expanded into its constituent Pauli matrix components as,

$$\begin{aligned}\tilde{\Sigma}(\mathbf{k}, \omega) &= \sum_{\alpha=0}^3 \Sigma_\alpha(\mathbf{k}, \omega)\tau_\alpha \\ &= \begin{pmatrix} \Sigma_0(\mathbf{k}, \omega) + \Sigma_3(\mathbf{k}, \omega), & \Sigma_1(\mathbf{k}, \omega) - i\Sigma_2(\mathbf{k}, \omega) \\ \Sigma_1(\mathbf{k}, \omega) + i\Sigma_2(\mathbf{k}, \omega), & \Sigma_0(\mathbf{k}, \omega) - \Sigma_3(\mathbf{k}, \omega) \end{pmatrix},\end{aligned}\quad (4)$$

with $\Sigma_0(\mathbf{k}, \omega)$ and $\Sigma_3(\mathbf{k}, \omega)$ that are respectively the antisymmetric and symmetric parts of the homogenous self-energy in the particle-hole channel, while $\Sigma_1(\mathbf{k}, \omega)$ and $\Sigma_2(\mathbf{k}, \omega)$ that are respectively the real and imaginary parts of the homogenous self-energy in the particle-particle channel. Moreover, these homogenous self-energies $\Sigma_0(\mathbf{k}, \omega)$, $\Sigma_1(\mathbf{k}, \omega)$, $\Sigma_2(\mathbf{k}, \omega)$, and $\Sigma_3(\mathbf{k}, \omega)$ have been derived explicitly in Ref. 53 in terms of the full charge-spin recombination. In particular, the sharp peaks visible for temperature $T \rightarrow 0$ in $\Sigma_0(\mathbf{k}, \omega)$, $\Sigma_1(\mathbf{k}, \omega)$, $\Sigma_2(\mathbf{k}, \omega)$, and $\Sigma_3(\mathbf{k}, \omega)$ are actually a δ -functions, broadened by a small damping used in the numerical calculation for a finite lattice. The calculation in this paper for $\Sigma_0(\mathbf{k}, \omega)$, $\Sigma_1(\mathbf{k}, \omega)$, $\Sigma_2(\mathbf{k}, \omega)$, and $\Sigma_3(\mathbf{k}, \omega)$ is performed numerically on a 120×120 lattice in momentum space, with the infinitesimal $i0_+ \rightarrow i\Gamma$ replaced by a small damping $\Gamma = 0.05J$.

The homogenous electron spectral function can be obtained directly from the above homogenous electron propagator (3). In this case, the topology of EFS in the pure system has been discussed in terms of the intensity map of the homogenous electron spectral function at zero energy^{61–63}, and the obtained results show that EFS contour is broken up into the disconnected Fermi arcs located around the nodal region^{36–43}, however, a large number of the low-energy electronic states is available at around the tips of the Fermi arcs, and then all the anomalous properties arise from these quasiparticle excitations located at around the tips of the Fermi arcs. In particular, these tips of the Fermi arcs connected by the scattering wave vectors \mathbf{q}_i naturally construct an *octet scattering model*, and then the quasiparticle scattering with the scattering wave vectors \mathbf{q}_i therefore contribute effectively to the quasiparticle scattering processes^{44–48}. Moreover, this *octet scattering model* can persist into the case for a finite binding-energy^{33–35}, which leads to that the sharp peaks in the ARPES autocorrelation spectrum with the scattering wave vectors \mathbf{q}_i are directly correlated to the regions of the highest joint density of states.

A. Impurity-dressed electron propagator

In the low-temperature limit, the framework for the discussions of the impurity-scattering effect is the self-consistent T -matrix approach^{3–6,64–66}. The discussions of the low-temperature microwave conductivity of cuprate superconductors in this paper builds on the impurity-dressed electron propagator, which is obtained from the dress of the homogenous electron propagator (3) via the impurity scattering⁴⁹, where the self-consistent T -matrix approach is employed to derive the impurity scattering self-energy in the Fermi-arc-tip approximation of the quasiparticle excitations and scattering processes. For a convenience in the following discussions of the microwave conductivity, a short summary of the derivation process of the impurity-dressed electron propagator⁴⁹ is therefore given in this subsection.

The homogenous electron propagator in Eq. (3) is dressed due to the presence of the impurity scattering^{3–6}, and can be expressed explicitly as,

$$\tilde{G}_I(\mathbf{k}, \omega)^{-1} = \tilde{G}(\mathbf{k}, \omega)^{-1} - \tilde{\Sigma}_I(\mathbf{k}, \omega),\quad (5)$$

where in a striking similarity to the homogenous self-energy (4), the impurity scattering self-energy $\tilde{\Sigma}_I(\mathbf{k}, \omega)$ can be also expanded into its constituent Pauli matrix components as,

$$\begin{aligned}\tilde{\Sigma}_I(\mathbf{k}, \omega) &= \sum_{\alpha=0}^3 \Sigma_{I\alpha}(\mathbf{k}, \omega)\tau_\alpha \\ &= \begin{pmatrix} \Sigma_{I0}(\mathbf{k}, \omega) + \Sigma_{I3}(\mathbf{k}, \omega), & \Sigma_{I1}(\mathbf{k}, \omega) - i\Sigma_{I2}(\mathbf{k}, \omega) \\ \Sigma_{I1}(\mathbf{k}, \omega) + i\Sigma_{I2}(\mathbf{k}, \omega), & \Sigma_{I0}(\mathbf{k}, \omega) - \Sigma_{I3}(\mathbf{k}, \omega) \end{pmatrix}.\end{aligned}\quad (6)$$

The above impurity scattering self-energy together with the dressed electron propagator (5) can be analyzed

in the self-consistent T -matrix approach^{64–66}, where $\tilde{\Sigma}_I(\mathbf{k}, \omega)$ can be derived approximately as,

$$\tilde{\Sigma}_I(\mathbf{k}, \omega) = n_i N \tilde{T}_{\mathbf{k}\mathbf{k}}(\omega), \quad (7)$$

with the impurity concentration n_i , the number of sites on a square lattice N , and the diagonal part of the T -matrix $\tilde{T}_{\mathbf{k}\mathbf{k}}(\omega)$, while the self-consistent T -matrix equation that can be expressed formally by the summation of all impurity scattering processes as,

$$\tilde{T}_{\mathbf{k}\mathbf{k}'} = \frac{1}{N} \tau_3 V_{\mathbf{k}\mathbf{k}'} + \frac{1}{N} \sum_{\mathbf{k}''} V_{\mathbf{k}\mathbf{k}''} \tau_3 \tilde{G}_I(\mathbf{k}'', \omega) \tilde{T}_{\mathbf{k}''\mathbf{k}'}, \quad (8)$$

where $V_{\mathbf{k}\mathbf{k}'}$ is the momentum dependence of the impurity scattering potential. It thus shows that the initial and final momenta of an impurity scattering event must always be equal to the momentum-space sited in the Brillouin zone (BZ).

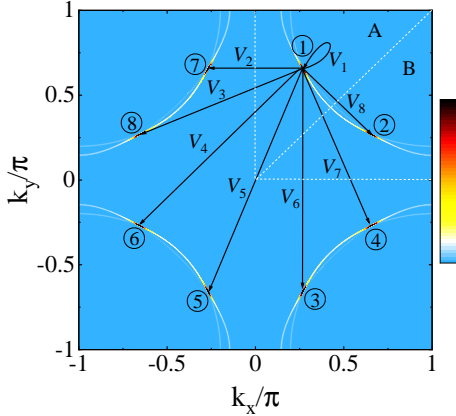


FIG. 1. (Color online) The impurity scattering in the microscopic octet scattering model, where V_1 is the impurity scattering potential for the intra-tip scattering, V_2 , V_3 , V_7 , and V_8 are the impurity scattering potentials for the adjacent-tip scattering, while V_4 , V_5 , and V_6 are the impurity scattering potentials for the opposite-tip scattering. In the d-wave superconducting-state, the tips of the Fermi arcs are divided into two groups: (A) the tips of the Fermi arcs located at the region of $|k_y| > |k_x|$ and (B) the tips of the Fermi arcs located at the region of $|k_x| > |k_y|$.

However, in the microscopic octet scattering model⁴⁹ shown in Fig. 1, a particularly large fraction of the spectral weight is accommodated at around eight tips of the Fermi arcs in the case of low temperatures and low energies, indicating that a large number of the quasiparticle excitations are induced only at around these eight tips of the Fermi arcs. On the other hand, the strength of the impurity scattering potential $V_{\mathbf{k}\mathbf{k}'}$ in the T -matrix equation (8) falls off quickly when the momentum shifts away from the tips of the Fermi arcs. In this case, the initial and final momenta of an impurity scattering event are always approximately equal to the momentum-space sited at around one of these eight tips of the Fermi arcs. In this Fermi-arc-tip approximation⁴⁹, we only need to consider

three possible cases as shown in Fig. 1 for the impurity scattering potential $V_{\mathbf{k}\mathbf{k}'}$ in the T -matrix equation (8): (i) the impurity scattering potential for the scattering process at the intra-tip of the Fermi arc $V_{\mathbf{k}\mathbf{k}'} = V_1$, where \mathbf{k} and \mathbf{k}' are located at the same tip of the Fermi arc; (ii) the impurity scattering potentials for the scattering process at the adjacent-tips of the Fermi arcs $V_{\mathbf{k}\mathbf{k}'} = V_2$, $V_{\mathbf{k}\mathbf{k}'} = V_3$, $V_{\mathbf{k}\mathbf{k}'} = V_7$, and $V_{\mathbf{k}\mathbf{k}'} = V_8$, where \mathbf{k} and \mathbf{k}' are located at the adjacent-tips of the Fermi arcs; (iii) the impurity scattering potentials for the scattering process at the opposite-tips of the Fermi arcs $V_{\mathbf{k}\mathbf{k}'} = V_4$, $V_{\mathbf{k}\mathbf{k}'} = V_5$, and $V_{\mathbf{k}\mathbf{k}'} = V_6$, where \mathbf{k} and \mathbf{k}' are located at the opposite-tips of the Fermi arcs, and then the impurity scattering potential $V_{\mathbf{k}\mathbf{k}'}$ in the self-consistent T -matrix equation (8) is reduced as a 8×8 -matrix,

$$\tilde{V} = \begin{pmatrix} V_{11} & V_{12} & \cdots & V_{18} \\ V_{21} & V_{22} & \cdots & V_{28} \\ \vdots & \vdots & \ddots & \vdots \\ V_{81} & V_{82} & \cdots & V_{88} \end{pmatrix}, \quad (9)$$

where the matrix elements are given by: $V_{jj} = V_1$ for $j = 1, 2, 3, \dots, 8$, $V_{jj'} = V_{j'j} = V_2$ for $j = 1, 2, 3, 6$ with the corresponding $j' = 7, 4, 5, 8$, respectively, $V_{jj'} = V_{j'j} = V_3$ for $j = 1, 2, 3, 4$ with the corresponding $j' = 8, 7, 6, 5$, respectively, $V_{jj'} = V_{j'j} = V_4$ for $j = 1, 2, 3, 4$ with the corresponding $j' = 6, 5, 8, 7$, respectively, $V_{jj'} = V_{j'j} = V_5$ for $j = 1, 2, 3, 4$ with the corresponding $j' = 5, 6, 7, 8$, respectively, $V_{jj'} = V_{j'j} = V_6$ for $j = 1, 2, 4, 5$ with the corresponding $j' = 3, 8, 6, 7$, respectively, $V_{jj'} = V_{j'j} = V_7$ for $j = 1, 2, 5, 6$ with the corresponding $j' = 4, 3, 8, 7$, respectively, and $V_{jj'} = V_{j'j} = V_8$, for $j = 1, 3, 5, 7$ with the corresponding $j' = 2, 4, 6, 8$, respectively.

With the help of the above impurity scattering potential matrix \tilde{V} , the self-consistent T -matrix equation (8) is reduced as a 16×16 -matrix equation around eight tips of the Fermi arcs as,

$$\tilde{T}_{jj'} = \frac{1}{N} \tau_3 V_{jj'} + \frac{1}{N} \sum_{j''\mathbf{k}''} V_{jj''} [\tau_3 \tilde{G}_I(\mathbf{k}'', \omega)] \tilde{T}_{j''j'}, \quad (10)$$

where j , j' , and j'' label the tips of the Fermi arcs, the summation \mathbf{k}'' is restricted within the area around the tip j'' of the Fermi arc, $\tilde{T}_{jj'}$ is now an impurity-average quantity, and then the impurity scattering self-energy $\tilde{\Sigma}_I(\mathbf{k}, \omega)$ in Eq. (7) is obtained as,

$$\tilde{\Sigma}_I(\omega) = n_i N \tilde{T}_{jj}(\omega). \quad (11)$$

It has been shown that the diagonal propagator in Eq. (5) is symmetrical about the nodal direction, while the off-diagonal propagator is asymmetrical about the nodal direction, since the SC-state has a d-wave symmetry⁴⁹. In this case, the region of the location of the tips of the Fermi arcs has been separated into two groups: (A) the tips of the Fermi arcs located at the region of $|k_y| > |k_x|$, and (B) the tips of the Fermi arcs located at the region of $|k_x| > |k_y|$, and then the dressed electron propagator

$\tilde{G}_I(\mathbf{k}, \omega)$ in Eq. (5) can be also derived in the regions A and B as⁴⁹,

$$\begin{aligned} \tilde{G}_I^{(A)}(\mathbf{k}, \omega) &= \frac{1}{F_I^{(A)}(\mathbf{k}, \omega)} \{ [\omega - \Sigma_0(\mathbf{k}, \omega) - \Sigma_{I0}(\omega)] \tau_0 \\ &+ [\Sigma_1(\mathbf{k}, \omega) + \Sigma_{I1}^{(A)}(\omega)] \tau_1 + [\Sigma_2(\mathbf{k}, \omega) + \Sigma_{I2}^{(A)}(\omega)] \tau_2 \\ &+ [\varepsilon_{\mathbf{k}} + \Sigma_3(\mathbf{k}, \omega) + \Sigma_{I3}(\omega)] \tau_3 \}, \end{aligned} \quad (12a)$$

$$\begin{aligned} \tilde{G}_I^{(B)}(\mathbf{k}, \omega) &= \frac{1}{F_I^{(B)}(\mathbf{k}, \omega)} \{ [\omega - \Sigma_0(\mathbf{k}, \omega) - \Sigma_{I0}(\omega)] \tau_0 \\ &+ [\Sigma_1(\mathbf{k}, \omega) + \Sigma_{I1}^{(B)}(\omega)] \tau_1 + [\Sigma_2(\mathbf{k}, \omega) + \Sigma_{I2}^{(B)}(\omega)] \tau_2 \\ &+ [\varepsilon_{\mathbf{k}} + \Sigma_3(\mathbf{k}, \omega) + \Sigma_{I3}(\omega)] \tau_3 \}, \end{aligned} \quad (12b)$$

respectively, where $F_I^{(A)}(\mathbf{k}, \omega) = [\omega - \Sigma_0(\mathbf{k}, \omega) - \Sigma_{I0}(\omega)]^2 - [\varepsilon_{\mathbf{k}} + \Sigma_3(\mathbf{k}, \omega) + \Sigma_{I3}(\omega)]^2 - [\Sigma_1(\mathbf{k}, \omega) + \Sigma_{I1}^{(A)}(\omega)]^2 - [\Sigma_2(\mathbf{k}, \omega) + \Sigma_{I2}^{(A)}(\omega)]^2$, $F_I^{(B)}(\mathbf{k}, \omega) = [\omega - \Sigma_0(\mathbf{k}, \omega) - \Sigma_{I0}(\omega)]^2 - [\varepsilon_{\mathbf{k}} + \Sigma_3(\mathbf{k}, \omega) + \Sigma_{I3}(\omega)]^2 - [\Sigma_1(\mathbf{k}, \omega) + \Sigma_{I1}^{(B)}(\omega)]^2 - [\Sigma_2(\mathbf{k}, \omega) + \Sigma_{I2}^{(B)}(\omega)]^2$. In the self-consistent T -matrix approach, these impurity scattering self-energies $\Sigma_{I0}^{(A)}(\omega)$ [$\Sigma_{I0}^{(B)}(\omega)$], $\Sigma_{I1}^{(A)}(\omega)$ [$\Sigma_{I1}^{(B)}(\omega)$], $\Sigma_{I2}^{(A)}(\omega)$ [$\Sigma_{I2}^{(B)}(\omega)$], and $\Sigma_{I3}^{(A)}(\omega)$ [$\Sigma_{I3}^{(B)}(\omega)$] and the related T -matrix $\tilde{T}_{jj'}^{(A)} = \sum_{\alpha} T_{Ajj'}^{(\alpha)} \tau_{\alpha}$ [$\tilde{T}_{jj'}^{(B)} = \sum_{\alpha} T_{Bjj'}^{(\alpha)} \tau_{\alpha}$] with the matrix elements $T_{Ajj'}^{(\alpha)}$ [$T_{Bjj'}^{(\alpha)}$] in Eq. (10) have been obtained in the Fermi-arc-tip approximation of the quasiparticle excitations and scattering processes, and given explicitly in Ref. 49.

With the help of the above dressed electron propagator (12) [then the dressed electron spectral function], we⁴⁹ have also discussed the influence of the impurity scattering on the electronic structure of cuprate superconductors, and the obtained results of the line-shape

in the quasiparticle excitation spectrum and the ARPES autocorrelation spectrum are well consistent with the corresponding experimental results^{33–35,67–73}.

B. Microwave Conductivity

Now we turn to derive the microscopic conductivity of cuprate superconductors in the presence of impurities, which is closely associated with the dressed electron propagator (12). The linear response theory allows one to obtain the microwave conductivity in terms of the Kubo formula⁶⁴,

$$\overleftrightarrow{\sigma}(\Omega, T) = -\frac{\text{Im}\overleftrightarrow{\Pi}(\Omega)}{\Omega}, \quad (13)$$

where $\overleftrightarrow{\Pi}(\Omega)$ is the retarded electron current-current correlation function, and can be expressed explicitly as,

$$\overleftrightarrow{\Pi}(i\Omega_m) = -\frac{1}{N} \int_0^{\beta} d\tau e^{i\Omega_m\tau} \langle T_{\tau} \mathbf{J}(\tau) \mathbf{J}(0) \rangle, \quad (14)$$

with $\beta = 1/T$, the bosonic Matsubara frequency $\Omega_m = 2\pi m/\beta$, and the current density of electrons \mathbf{J} . This current density of electrons can be obtained in terms of the electron polarization operator, which is a summation over all the particles and their positions⁶⁴, and can be expressed explicitly in the fermion-spin representation (2) as $\mathbf{P} = \sum_{l\sigma} \mathbf{R}_l \hat{C}_{l\sigma}^{\dagger} \hat{C}_{l\sigma} = \frac{1}{2} \sum_{l\sigma} \mathbf{R}_l h_{l\sigma} h_{l\sigma}^{\dagger}$. Within the t - J model (1) in the fermion-spin representation (2), the current density of electrons is obtained by evaluating the time-derivative of the polarization operator using the Heisenberg's equation of motion as,

$$\begin{aligned} \mathbf{J} &= -ie[H, \mathbf{P}] = -i\frac{1}{2}et \sum_{\langle l\hat{n} \rangle} \hat{\eta} (h_{l+\hat{n}\uparrow}^{\dagger} h_{l\uparrow} S_l^+ S_{l+\hat{n}}^- + h_{l+\hat{n}\downarrow}^{\dagger} h_{l\downarrow} S_l^- S_{l+\hat{n}}^+) + i\frac{1}{2}et' \sum_{\langle l\hat{n}' \rangle} \hat{\eta}' (h_{l+\hat{n}'\uparrow}^{\dagger} h_{l\uparrow} S_l^+ S_{l+\hat{n}'}^- + h_{l+\hat{n}'\downarrow}^{\dagger} h_{l\downarrow} S_l^- S_{l+\hat{n}'}^+) \\ &= i\frac{1}{2}et \sum_{\langle l\hat{n} \rangle \sigma} \hat{\eta} C_{l\sigma}^{\dagger} C_{l+\hat{n}\sigma} - i\frac{1}{2}et' \sum_{\langle l\hat{n}' \rangle \sigma} \hat{\eta}' C_{l\sigma}^{\dagger} C_{l+\hat{n}'\sigma} \approx -eV_F \sum_{\mathbf{k}\sigma} C_{\mathbf{k}\sigma}^{\dagger} C_{\mathbf{k}\sigma}, \end{aligned} \quad (15)$$

with the electron charge e , the electron Fermi velocity V_F , which can be derived directly from the energy dispersion $\varepsilon_{\mathbf{k}}$ in the tight-binding approximation in Eq. (3) as,

$$\mathbf{V}_F = V_F^{(x)} \hat{k}_x + V_F^{(y)} \hat{k}_y = V_F [\hat{k}_x \cos \theta_{\mathbf{k}_F} + \hat{k}_y \sin \theta_{\mathbf{k}_F}], \quad (16)$$

where $V_F^{(x)} = t \sin k_F^{(x)} - 2t' \sin k_F^{(x)} \cos k_F^{(y)}$, $V_F^{(y)} = t \sin k_F^{(y)} - 2t' \sin k_F^{(y)} \cos k_F^{(x)}$, $\cos \theta_{\mathbf{k}_F} = V_F^{(x)}/V_F$, $\sin \theta_{\mathbf{k}_F} = V_F^{(y)}/V_F$, and $V_F = \sqrt{[V_F^{(x)}]^2 + [V_F^{(y)}]^2}$. For a convenience in the following discussions of the electron

current-current correlation function (14), the electron operators can be rewritten in the Nambu representation as $\Psi_{\mathbf{k}}^{\dagger} = (C_{\mathbf{k}\uparrow}^{\dagger}, C_{-\mathbf{k}\downarrow})$ and $\Psi_{\mathbf{k}} = (C_{\mathbf{k}\uparrow}, C_{-\mathbf{k}\downarrow}^{\dagger})^T$, and then the current density of electrons in Eq. (15) can be rewritten in the Nambu representation as,

$$\mathbf{J} = -eV_F \sum_{\mathbf{k}} \Psi_{\mathbf{k}}^{\dagger} \tau_0 \Psi_{\mathbf{k}}. \quad (17)$$

With the help of the above current density of electrons (17), the impurity-induced vertex-corrected current-current correlation function (14) can be formally expressed in terms of the dressed electron propagator as,

$$\overleftrightarrow{\Pi}(i\Omega_m) = \frac{1}{N} \int_0^\beta d\tau e^{i\Omega_m \tau} \overleftrightarrow{\Pi}(\tau) = (eV_F)^2 \frac{1}{N} \sum_{\mathbf{k}} \frac{1}{\beta} \sum_{i\omega_n} \hat{\mathbf{k}} Tr[\tilde{G}_I(\mathbf{k}, i\omega_n) \tilde{G}_I(\mathbf{k}, i\omega_n + i\Omega_m) \tilde{\Gamma}(\mathbf{k}, i\omega_n, i\Omega_m)], \quad (18)$$

where $\omega_n = (2n + 1)\pi/\beta$ is the fermionic Matsubara frequency, while the impurity-induced vertex correction in the ladder approximation can be generally expressed as⁶⁴,

$$\tilde{\Gamma}(\mathbf{k}, i\omega_n, i\Omega_m) = \hat{\mathbf{k}}\tau_0 + n_i N \sum_{\mathbf{k}''} \tilde{T}_{\mathbf{k}\mathbf{k}''}(i\omega_n + i\Omega_m) \tilde{G}_I(\mathbf{k}'', i\omega_n + i\Omega_m) \tilde{\Gamma}(\mathbf{k}'', i\omega_n, i\Omega_m) \tilde{G}_I(\mathbf{k}'', i\omega_n) \tilde{T}_{\mathbf{k}''\mathbf{k}}(i\omega_n). \quad (19)$$

Starting from the homogenous part of the d-wave BCS type formalism, the effect of the impurity scattering on the microwave conductivity has been discussed in the self-consistent T -matrix approach by taking into account the impurity-induced vertex correction²⁶⁻³¹, where the vertex-corrected electron current-current correlation function and the related impurity-dressed electron propagator have been evaluated in the *nodal approximation*. In the following discussions, the vertex-corrected electron current-current correlation function is generalized from the previous case obtained in the *nodal approximation*²⁶⁻³¹ to the present case in the *Fermi-arc-tip approximation*, where the impurity-induced vertex correction for the electron current-current correlation function (19) can be expressed explicitly in the regions A and B as,

$$\tilde{\Gamma}^{(A)}(\mathbf{k}, i\omega_n, i\Omega_m) = \hat{k}_F^{(j)} \tau_0 + \hat{k}_x^{(j)} \tilde{\Lambda}_x^{(A)}(i\omega_n, i\Omega_m) + \hat{k}_y^{(j)} \tilde{\Lambda}_y^{(A)}(i\omega_n, i\Omega_m), \quad \text{for } j \in \text{odd}, \quad (20a)$$

$$\tilde{\Gamma}^{(B)}(\mathbf{k}, i\omega_n, i\Omega_m) = \hat{k}_F^{(j)} \tau_0 + \hat{k}_x^{(j)} \tilde{\Lambda}_x^{(B)}(i\omega_n, i\Omega_m) + \hat{k}_y^{(j)} \tilde{\Lambda}_y^{(B)}(i\omega_n, i\Omega_m), \quad \text{for } j \in \text{even}, \quad (20b)$$

respectively, while the vertex kernels $\tilde{\Lambda}_x^{(A)}(i\omega_n, i\Omega_m)$, $\tilde{\Lambda}_y^{(A)}(i\omega_n, i\Omega_m)$, $\tilde{\Lambda}_x^{(B)}(i\omega_n, i\Omega_m)$, and $\tilde{\Lambda}_y^{(B)}(i\omega_n, i\Omega_m)$ satisfy the following self-consistent equations,

$$\begin{aligned} \hat{k}_x^{(j)} \tilde{\Lambda}_x^{(A)}(i\omega_n, i\Omega_m) + \hat{k}_y^{(j)} \tilde{\Lambda}_y^{(A)}(i\omega_n, i\Omega_m) = n_i N \{ & \sum_{\substack{\mathbf{k} \in A \\ j'' \in \text{odd}}} \tilde{T}_{jj''}(i\omega_n + i\Omega_m) \tilde{G}_I^{(A)}(\mathbf{k}, i\omega_n + i\Omega_m) \\ & \times [\hat{k}_F^{(j'')} \tau_0 + \hat{k}_x^{(j'')} \tilde{\Lambda}_x^{(A)}(i\omega_n, i\Omega_m) + \hat{k}_y^{(j'')} \tilde{\Lambda}_y^{(A)}(i\omega_n, i\Omega_m)] \tilde{G}_I^{(A)}(\mathbf{k}, i\omega_n) \tilde{T}_{j''j}(i\omega_n) \\ & + \sum_{\substack{\mathbf{k} \in B \\ j'' \in \text{even}}} \tilde{T}_{jj''}(i\omega_n + i\Omega_m) \tilde{G}_I^{(B)}(\mathbf{k}, i\omega_n + i\Omega_m) [\hat{k}_F^{(j'')} \tau_0 + \hat{k}_x^{(j'')} \tilde{\Lambda}_x^{(B)}(i\omega_n, i\Omega_m) \\ & + \hat{k}_y^{(j'')} \tilde{\Lambda}_y^{(B)}(i\omega_n, i\Omega_m)] \tilde{G}_I^{(B)}(\mathbf{k}, i\omega_n) \tilde{T}_{j''j}(i\omega_n) \}, \quad \text{for } j \in \text{odd}, \end{aligned} \quad (21a)$$

$$\begin{aligned} \hat{k}_x^{(j)} \tilde{\Lambda}_x^{(B)}(i\omega_n, i\Omega_m) + \hat{k}_y^{(j)} \tilde{\Lambda}_y^{(B)}(i\omega_n, i\Omega_m) = n_i N \{ & \sum_{\substack{\mathbf{k} \in A \\ j'' \in \text{odd}}} \tilde{T}_{jj''}(i\omega_n + i\Omega_m) \tilde{G}_I^{(A)}(\mathbf{k}, i\omega_n + i\Omega_m) \\ & \times [\hat{k}_F^{(j'')} \tau_0 + \hat{k}_x^{(j'')} \tilde{\Lambda}_x^{(A)}(i\omega_n, i\Omega_m) + \hat{k}_y^{(j'')} \tilde{\Lambda}_y^{(A)}(i\omega_n, i\Omega_m)] \tilde{G}_I^{(A)}(\mathbf{k}, i\omega_n) \tilde{T}_{j''j}(i\omega_n) \\ & + \sum_{\substack{\mathbf{k} \in B \\ j'' \in \text{even}}} \tilde{T}_{jj''}(i\omega_n + i\Omega_m) \tilde{G}_I^{(B)}(\mathbf{k}, i\omega_n + i\Omega_m) [\hat{k}_F^{(j'')} \tau_0 + \hat{k}_x^{(j'')} \tilde{\Lambda}_x^{(B)}(i\omega_n, i\Omega_m) \\ & + \hat{k}_y^{(j'')} \tilde{\Lambda}_y^{(B)}(i\omega_n, i\Omega_m)] \tilde{G}_I^{(B)}(\mathbf{k}, i\omega_n) \tilde{T}_{j''j}(i\omega_n) \}, \quad \text{for } j \in \text{even}. \end{aligned} \quad (21b)$$

Substituting the above results in Eq. (21) into Eqs. (19) and (18), the vertex-corrected electron current-current correlation function (18) now can be expressed as,

$$\begin{aligned} \overleftrightarrow{\Pi}(i\Omega_m) &= (eV_F^{(\text{TFA})})^2 \frac{1}{N} \sum_{\mathbf{k}} \frac{1}{\beta} \sum_{i\omega_n} (\hat{k}_x + \hat{k}_y) Tr \{ \tilde{G}_I(\mathbf{k}, i\omega_n) \tilde{G}_I(\mathbf{k}, i\omega_n + i\Omega_m) [\hat{k}_F \tau_0 + \hat{k}_x \tilde{\Lambda}_x(i\omega_n, i\Omega_m) + \hat{k}_y \tilde{\Lambda}_y(i\omega_n, i\Omega_m)] \} \\ &= (eV_F^{(\text{TFA})})^2 \sum_{j \in \text{odd}} \frac{1}{\beta} \sum_{i\omega_n} (\hat{k}_x^{(j)} + \hat{k}_y^{(j)}) Tr \left\{ \frac{1}{N} \sum_{\mathbf{k} \in A} \tilde{G}_I^{(A)}(\mathbf{k}, i\omega_n) \tilde{G}_I^{(A)}(\mathbf{k}, i\omega_n + i\Omega_m) [\hat{k}_F^{(j)} \tau_0 + \hat{k}_x^{(j)} \tilde{\Lambda}_x^{(A)}(i\omega_n, i\Omega_m) \right. \\ &+ \hat{k}_y^{(j)} \tilde{\Lambda}_y^{(A)}(i\omega_n, i\Omega_m)] \} + (eV_F^{(\text{TFA})})^2 \sum_{j \in \text{even}} \frac{1}{\beta} \sum_{i\omega_n} (\hat{k}_x^{(j)} + \hat{k}_y^{(j)}) Tr \left\{ \frac{1}{N} \sum_{\mathbf{k} \in B} \tilde{G}_I^{(B)}(\mathbf{k}, i\omega_n) \tilde{G}_I^{(B)}(\mathbf{k}, i\omega_n + i\Omega_m) \right. \\ &\times [\hat{k}_F^{(j)} \tau_0 + \hat{k}_x^{(j)} \tilde{\Lambda}_x^{(B)}(i\omega_n, i\Omega_m) + \hat{k}_y^{(j)} \tilde{\Lambda}_y^{(B)}(i\omega_n, i\Omega_m)] \}, \end{aligned} \quad (22)$$

with the electron Fermi velocity $V_F^{(\text{TFA})}$ at around the tips of the Fermi arcs. However, in the absence of an external magnetic field, the rotational symmetry in the system is unbroken, indicating that $\Pi_{xy}(\Omega) = \Pi_{yx}(\Omega) = 0$ and

$\Pi_{xx}(\Omega) = \Pi_{yy}(\Omega)$, and then the above vertex-corrected electron current-current correlation function (22) is reduced as,

$$\overleftrightarrow{\Pi}(i\Omega_m) = \begin{pmatrix} \Pi_{xx}(i\Omega_m) & 0 \\ 0 & \Pi_{yy}(i\Omega_m) \end{pmatrix} = \tau_0 \Pi_{xx}(i\Omega_m), \quad (23)$$

where $\Pi_{xx}(i\Omega_m)$ is given by,

$$\Pi_{xx}(i\Omega_m) = (2eV_F^{(\text{TFA})})^2 \frac{1}{\beta} \sum_{i\omega_n} J_{xx}(i\omega_n, i\omega_n + i\Omega_m), \quad (24)$$

with the kernel function,

$$\begin{aligned} J_{xx}(i\omega_n, i\omega_n + i\Omega_m) &= \frac{1}{N} \sum_{\alpha=0}^3 \left\{ \cos^2 \theta_F^{(\text{A})} \tilde{I}_0^{(\text{A})}(\alpha, i\omega_n, i\omega_n + i\Omega_m) \text{Tr}[\tau_\alpha[\tau_0 + \tilde{\Lambda}_x^{(\text{A})}(i\omega_n, i\Omega_m)]] \right. \\ &\quad \left. + \cos^2 \theta_F^{(\text{B})} \tilde{I}_0^{(\text{B})}(\alpha, i\omega_n, i\omega_n + i\Omega_m) \text{Tr}[\tau_\alpha[\tau_0 + \tilde{\Lambda}_x^{(\text{B})}(i\omega_n, i\Omega_m)]] \right\}, \end{aligned} \quad (25)$$

where the functions $\tilde{I}_0^{(\text{A})}(\alpha, i\omega_n, i\omega_n + i\Omega_m)$ and $\tilde{I}_0^{(\text{B})}(\alpha, i\omega_n, i\omega_n + i\Omega_m)$ are defined as,

$$\sum_{\mathbf{k} \in \text{A}} \tilde{G}_1^{(\text{A})}(\mathbf{k}, i\omega_n) \tau_\gamma \tilde{G}_1^{(\text{A})}(\mathbf{k}, i\omega_n + i\Omega_m) = \sum_{\beta=0}^3 \tilde{I}_\gamma^{(\text{A})}(\beta, i\omega_n, i\omega_n + i\Omega_m) \tau_\beta, \quad (26a)$$

$$\sum_{\mathbf{k} \in \text{B}} \tilde{G}_1^{(\text{B})}(\mathbf{k}, i\omega_n) \tau_\gamma \tilde{G}_1^{(\text{B})}(\mathbf{k}, i\omega_n + i\Omega_m) = \sum_{\beta=0}^3 \tilde{I}_\gamma^{(\text{B})}(\beta, i\omega_n, i\omega_n + i\Omega_m) \tau_\beta, \quad (26b)$$

respectively. After a quite complicated calculation, the function $\text{Tr}[\tau_\alpha \tilde{\Lambda}_x^{(\text{A})}(\omega, \Omega)]$ in the above kernel function (25), which is a trace of the product of the vertex kernel $\tilde{\Lambda}_x^{(\text{A})}(\omega, \Omega)$ and matrix τ_α with $\alpha = 0, 1, 2, 3$ in the region A of BZ, and the function $\text{Tr}[\tau_\alpha \tilde{\Lambda}_x^{(\text{B})}(\omega, \Omega)]$ in the above kernel function (25), which is a trace of the product of the vertex kernel $\tilde{\Lambda}_x^{(\text{B})}(\omega, \Omega)$ and matrix τ_α in the region B of BZ, can be derived straightforwardly [see Appendix A], and then the above kernel function $J_{xx}(\omega, \omega + \Omega)$ can be obtained explicitly.

On the other hand, the dressed electron propagators $\tilde{G}_1(\mathbf{k}, i\omega_n)$ and $\tilde{G}_1(\mathbf{k}, i\omega_n + i\Omega_m)$ are involved directly in the above kernel function $J_{xx}(i\omega_n, i\omega_n + i\Omega_m)$ in Eq. (25), then the singularity of $J_{xx}(i\omega_n, i\omega_n + i\Omega_m)$ only lies at the real axes [$\epsilon \in \mathbb{R}$] and these parallel to the real axes [$\epsilon - i\Omega_m$]. In this case, the contribution for the summation of the kernel function $J_{xx}(i\omega_n, i\omega_n + i\Omega_m)$ in Eq. (24) over the fermionic Matsubara frequency $i\omega_n$ comes from the two branch cuts: $\epsilon \in \mathbb{R}$ and $\epsilon - i\Omega_m$, and then the vertex-corrected electron current-current correlation function (24) can be expressed as,

$$\begin{aligned} \Pi_{xx}(i\Omega_m) &= i(2eV_F^{(\text{TFA})})^2 \int_{-\infty}^{\infty} \frac{d\epsilon}{2\pi} n_F(\epsilon) [J_{xx}(\epsilon + i\delta, \epsilon + i\Omega_m) - J_{xx}(\epsilon - i\delta, \epsilon + i\Omega_m) \\ &\quad + J_{xx}(\epsilon - i\Omega_m, \epsilon + i\delta) - J_{xx}(\epsilon - i\Omega_m, \epsilon - i\delta)], \end{aligned} \quad (27)$$

By virtue of the analytical continuation $i\Omega_m \rightarrow \Omega + i\delta$, the above vertex-corrected electron current-current correlation function (27) can be obtained explicitly as,

$$\begin{aligned} \Pi_{xx}(\Omega) &= i(2eV_F^{(\text{TFA})})^2 \int_{-\infty}^{\infty} \frac{d\epsilon}{2\pi} \left\{ n_F(\epsilon) [J_{xx}(\epsilon + i\delta, \epsilon + \Omega + i\delta) - J_{xx}(\epsilon - i\delta, \epsilon + \Omega + i\delta)] \right. \\ &\quad \left. + n_F(\epsilon + \Omega) [J_{xx}(\epsilon - i\delta, \epsilon + \Omega + i\delta) - J_{xx}(\epsilon - i\delta, \epsilon + \Omega - i\delta)] \right\}, \end{aligned} \quad (28)$$

and then the microwave conductivity $\overleftrightarrow{\sigma}(\Omega, T) = \tau_0 \sigma(\Omega, T)$ in Eq. (13) in the presence of impurities is obtained as,

$$\sigma(\Omega) = -\frac{\text{Im}\Pi_{xx}(\Omega)}{\Omega} = (2eV_F^{(\text{TFA})})^2 \int_{-\infty}^{\infty} \frac{d\epsilon}{2\pi} \frac{n_F(\epsilon) - n_F(\epsilon + \Omega)}{\Omega} [\text{Re}J_{xx}(\epsilon - i\delta, \epsilon + \Omega + i\delta) - \text{Re}J_{xx}(\epsilon + i\delta, \epsilon + \Omega + i\delta)]. \quad (29)$$

III. QUANTITATIVE CHARACTERISTICS

In the self-consistent T -matrix approach, the strength of the impurity scattering potential is an important pa-

rameter. Unless otherwise indicated, the adjacent-tip im-

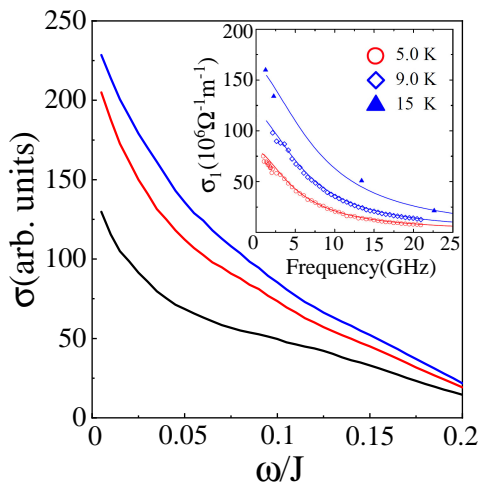


FIG. 2. (Color online) The microwave conductivity as a function of energy at the doping concentration $\delta = 0.15$ for temperatures $T = 0.005J \sim 5\text{K}$ (black-line), $T = 0.009J \sim 9\text{K}$ (red-line), and $T = 0.015J \sim 15\text{K}$ (blue-line) together with the impurity concentration $n_i = 0.0025$ and parameter of the impurity scattering potential strength $d = 0.05$. Inset: the corresponding experimental result of the microwave conductivity observed on $\text{YBa}_2\text{Cu}_3\text{O}_{6.993}$ taken from Ref. 20.

purity scattering $V_2, V_3, V_7,$ and V_8 , and the opposite-tip impurity scattering $V_4, V_5,$ and V_6 in the following discussions are chosen as $V_2 = 0.85V_1, V_3 = 0.8V_1, V_7 = 0.8V_1, V_8 = 0.9V_1, V_4 = 0.7V_1, V_5 = 0.65V_1,$ and $V_6 = 0.75V_1,$ respectively, as in the previous discussions of the influence of the impurity scattering on the electronic structure⁴⁹, while the strength of the intra-tip impurity scattering V_1 is chosen as $V_1 = V_{\text{scale}}\tan(\frac{\pi}{2}d)$ with $V_{\text{scale}} = 58J$ and the adjustable parameter d of the impurity scattering potential strength, where the case of $d \sim 0$ [then $\tan(\frac{\pi}{2}d) \sim 0$] is corresponding to the case $V_j \sim 0$ with $j = 1, 2, 3, \dots, 8$ in the Born-limit, while the case of $d \sim 1$ [then $\tan(\frac{\pi}{2}d) \sim \infty$] is corresponding to the case $V_j \sim \infty$ in the unitary-limit.

We are now ready to discuss the effect of the impurity scattering on the microwave conductivity in cuprate superconductors. We have performed a calculation for the microwave conductivity $\sigma(\omega, T)$ in Eq. (29), and the results of the microwave conductivity $\sigma(\omega, T)$ as a function of energy at the doping concentration $\delta = 0.15$ for temperatures $T = 0.005J \sim 5\text{K}$ (black-line), $T = 0.009J \sim 9\text{K}$ (red-line), and $T = 0.015J \sim 15\text{K}$ (blue-line) together with the impurity concentration $n_i = 0.0025$ and parameter of the impurity scattering potential strength $d = 0.05$ are plotted in Fig. 2 in comparison with the corresponding experimental results of the microwave conductivity observed on the cuprate superconductor²⁰ $\text{YBa}_2\text{Cu}_3\text{O}_{6.993}$ (inset). The results in Fig. 2 therefore show clearly that the energy dependence of the low-temperature microwave conductivity in cuprate superconductor¹⁶⁻²⁰ is qualitatively reproduced, where the highly unconventional features of the

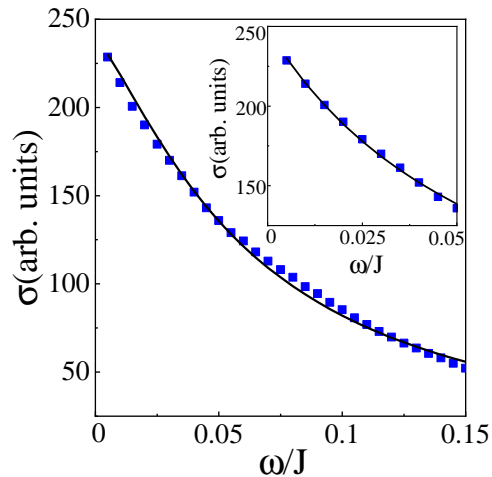


FIG. 3. (Color online) The numerical fit (black-line) with Eq. (30). The blue-squares are the result of the microwave conductivity with $T = 0.015J \sim 15\text{K}$ taken from Fig. 2. Inset: The numerical fit (black-line) with the fit form $\sigma(\omega, T) = A_0/[\omega + B_0]$, where $A_0 = 15.676$ and $B_0 = 0.063$. The blue-squares are the result of the low-energy microwave conductivity with $T = 0.015J \sim 15\text{K}$ taken from Fig. 2.

low-temperature microwave conductivity spectrum can be summarized as: (i) a sharp cusp-like peak develops at the low-energy limit; (ii) the low-temperature microwave conductivity spectrum is non-Drude-like; (iii) a high-energy tail falls slowly with the increase of energy. To see this non-Drude behavior in the low-temperature microwave conductivity spectrum more clearly, the results of the low-temperature microwave conductivity spectra shown in Fig. 2 have been numerically fitted in terms of the following fit form,

$$\sigma(\omega, T) = \frac{\sigma_0}{1 + (\omega/C_0T)^y}, \quad (30)$$

as they have been done in the experiments¹⁹, and the fit result at the temperature $T = 0.015J \sim 15\text{K}$ is plotted in Fig. 3 (black-line), where the fit parameters $\sigma_0 = 238.073, C_0 = 4.145,$ and $y = 1.333$. For a more better understanding, we have also fitted the low-energy part of the microwave conductivity spectrum alone with the fit form $\sigma(\omega, T) = A_0/[\omega + B_0]$, and the numerically fit result at the same temperature $T = 0.015J \sim 15\text{K}$ is also plotted in Fig. 3 (inset), where the fit parameters $A_0 = 15.676$ and $B_0 = 0.063$. These fit results in Fig. 3 thus indicate clearly that although the lower-energy cusp-like peak in Fig. 2 decay as $\rightarrow 1/[\omega + B_0]$, the overall shape of the low-temperature microwave conductivity spectrum in Fig. 2 exhibits a special non-Drude-like behavior, which can be well fitted by the formula in Eq. (30), in agreement with the corresponding experimental observations^{19,20}. More specifically, in comparison with other fit results at the temperatures $T = 0.005J \sim 5\text{K}$ and $T = 0.009J \sim 9\text{K}$, we also find that the fit parameter y in the fit form (30) is almost independence of tempera-

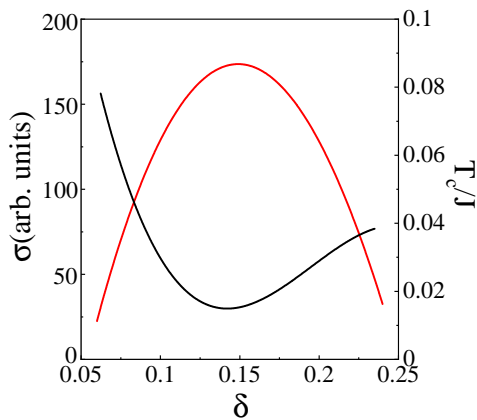


FIG. 4. (Color online) The microwave conductivity (black-line) as a function of doping with $T = 0.002J$ for $\omega = 0.0025J$ together with $n_i = 0.0025$ and $d = 0.05$. The red-line is the corresponding result of T_c .

ture, and remains relatively constant, taking the average value of $y = 1.333$. This anticipated value of the fit parameter $y = 1.333$ is not too far from the corresponding value of $y = 1.45(\pm 0.06)$, which has been employed in Ref. 19 to fit the corresponding experimental data with the same fit formula (30). The qualitative agreement between the present theoretical results and experimental data therefore also show that the kinetic-energy-driven superconductivity, incorporating the effect of the impurity scattering within the framework of the self-consistent T -matrix theory, can give a consistent description of the low-temperature microwave conductivity spectrum found in the microwave surface impedance measurements on cuprate superconductors^{16–20}.

As a natural consequence of the doped Mott insulator, the microwave conductivity in cuprate superconductors evolve with doping. In Fig. 4, we plot the result of $\sigma(\omega, T)$ [black-line] as a function of doping with $T = 0.002J$ for energy $\omega = 0.0025J$ together with $n_i = 0.0025$ and $d = 0.05$. For a comparison, the corresponding result^{51–53} of T_c obtained within the framework of the kinetic-energy-driven superconductivity is also shown in Fig. 4 (red-line). Apparently, in a striking contrast to the dome-like shape of the doping dependence of T_c , the microwave conductivity exhibits a reverse dome-like shape of the doping dependence, where $\sigma(\omega, T)$ is a decreasing function of the doping concentration, the system is thought to be at the underdoped regime. The system is at around the *optimal doping*, where $\sigma(\omega, T)$ reaches its minimum. However, with the further increase in the doping concentration, $\sigma(\omega, T)$ increases at the overdoped regime. This reverse dome-like shape of the doping dependence of the microwave conductivity in low energies and low temperatures is also qualitatively consistent with the microwave conductivity $\sigma_{ul} \propto 1/\bar{\Delta}$ in the universal limit of $\omega \rightarrow 0$ and $T \rightarrow 0$, since the SC gap parameter $\bar{\Delta}$ obtained within the framework of the kinetic-energy-driven superconductivity^{51–53} has the similar dome-like

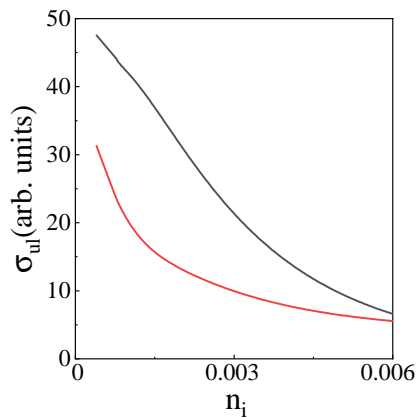


FIG. 5. (Color online) The microscopic conductivity in the universal-limit as a function of the impurity concentration at $\delta = 0.15$ with $T = 0.002J$ for $d = 0.05$ (black-line) and $d = 0.5$ (red-line).

shape of the doping dependence.

For a further understanding of the intrinsic effect of the impurity scattering on the SC-state quasiparticle transport in cuprate superconductors, we now turn to discuss the evolution of the microwave conductivity with the impurity concentration in the case of the universal-limit. The microwave conductivity σ_{ul} in the universal-limit can be obtained directly from the energy and temperature dependence of the microwave conductivity (29) in the zero-temperature ($T \rightarrow 0$) and zero-energy ($\Omega \rightarrow 0$) limits as,

$$\begin{aligned} \sigma_{ul} &= \lim_{\substack{\Omega \rightarrow 0 \\ T \rightarrow 0}} \sigma_{xz}(\Omega) \\ &= \frac{(2eV_F^{(\text{TFA})})^2}{2\pi} \lim_{\epsilon \rightarrow 0} [\text{Re}J_{xx}(\epsilon - i\delta, \epsilon + i\delta) \\ &\quad - \text{Re}J_{xx}(\epsilon + i\delta, \epsilon + i\delta)]. \end{aligned} \quad (31)$$

In this case, we have made a series of calculations for σ_{ul} at different impurity concentrations and different strengths of the impurity scattering potential, and the results of σ_{ul} as a function of the impurity concentration n_i at $\delta = 0.15$ for $d = 0.05$ (black-line) and $d = 0.5$ (red-line) are plotted in Fig. 5, where the main features can be summarized as: (i) for a given set of the impurity scattering potential strength, the microwave conductivity gradually decreases with the increase of the impurity concentration; (ii) for a given impurity concentration, the microwave conductivity decreases when the strength of the impurity scattering potential is increased. In other words, the crucial role played by the impurity scattering is the further reduction of the microwave conductivity.

In the present theoretical framework, the effect of the strong electron correlation on the microwave conductivity is reflected in the homogenous part of the electron propagator (then the homogenous self-energy), while the effect of the impurity scattering on the microwave conductivity is reflected both in the impurity-dressed electron prop-

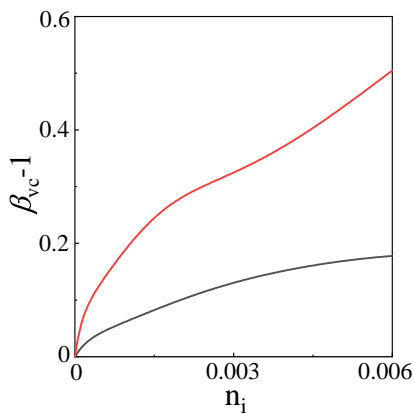


FIG. 6. (Color online) The characteristic factor of the impurity-induced vertex correction as a function of the impurity concentration at $\delta = 0.15$ for $d = 0.05$ (black-line) and $d = 0.5$ (red-line).

$$\sigma_{\text{ul}}^{(0)} = \frac{(2eV_{\text{F}}^{\text{(TFA)}})^2}{\pi} \lim_{\epsilon \rightarrow 0} \sum_{\mu=A,B} \Theta^{(\mu)}(\theta_{\text{F}}) \text{Re}[\tilde{I}_0^{(\mu)}(0, \epsilon - i\delta, \epsilon + i\delta) - \tilde{I}_0^{(\mu)}(0, \epsilon + i\delta, \epsilon + i\delta)], \quad (33)$$

with the function,

$$\Theta^{(\mu)}(\theta_{\text{F}}) = \begin{cases} \cos \theta_{\text{F}}^{(A)}, & \text{for } \mu = A \\ \cos \theta_{\text{F}}^{(B)}, & \text{for } \mu = B \end{cases} \quad (34)$$

In Fig. 6, we plot characteristic factor $\beta_{\text{vc}} - 1$ as a function of the impurity concentration n_i at $\delta = 0.15$ for $d = 0.05$ (black-line) and $d = 0.5$ (red-line), where for a given set of the impurity scattering potential strength, the characteristic factor monotonically *increases* as the impurity concentration is increased. On the other hand, for a given impurity concentration, $\beta_{\text{vc}} - 1$ *increases* with the increase of the strength of the impurity scattering potential. It thus shows clearly that the impurity-induced vertex correction is quite significant in the renormalization of the microwave conductivity^{26–32}, and then all the effects of the strong electron correlation, the impurity-scattering self-energy, and the impurity-induced vertex correction lead to the highly unconventional behaviors in the microwave conductivity of cuprate superconductors^{16–20}.

IV. SUMMARY

Starting from the homogenous electron propagator and the related microscopic octet scattering model, which are obtained within the framework of the kinetic-energy-driven superconductivity, we have re-derived the impurity-dressed electron propagator in the self-consistent T -matrix approach, where the impurity

agator (then the impurity-scattering self-energy) and the impurity-induced vertex correction to the electron current-current correlation function. In other words, the microwave conductivity is further renormalized by the impurity-induced vertex correction. For the understanding of this renormalization of the microwave conductivity from the impurity-induced vertex correction, the microwave conductivity in the case of the universal-limit in Eq. (31) can be rewritten as,

$$\sigma_{\text{ul}} = \beta_{\text{vc}} \sigma_{\text{ul}}^{(0)}, \quad (32)$$

where the characteristic factor β_{vc} is the impurity-induced vertex correction to the universal bare result of the microscopic conductivity $\sigma_{\text{ul}}^{(0)}$, while this $\sigma_{\text{ul}}^{(0)}$ can be reduced directly from σ_{ul} in Eq. (31) by ignoring the impurity-induced vertex correction as,

scattering self-energy is evaluated in the Fermi-arc-tip approximation of the quasiparticle excitations and scattering processes, and then the impurity-dressed electron propagator incorporates both the strong electron correlation and impurity-scattering effects. By virtue of this impurity-dressed electron propagator, we then have investigated the effect of the impurity scattering on the low-temperature microwave conductivity of cuprate superconductors, where the electron current-current correlation function is derived by taking into account the impurity-induced vertex correction. The obtained results show clearly that the low-temperature microwave conductivity spectrum is a non-Drude-like, with a sharp cusp-like peak extending to zero-energy and a high-energy tail falling slowly with energy, in agreement with the corresponding experimental observations^{16–20}. In particular, although the low-energy cusp-like peak decay as $\rightarrow A_0/[\omega + B_0]$, the overall shape of the low-temperature microwave conductivity spectrum exhibits a special non-Drude-like behavior, and can be well fitted by the formula $\sigma(\omega, T) = \sigma_0/[1 + (\omega/C_0T)^y]$ with the relatively temperature-independent constant y . Moreover, the low-temperature microwave conductivity decreases with the increase of the impurity concentration or with the increase of the strength of the impurity scattering potential. Our results therefore indicate that the highly unconventional features of the microwave conductivity in cuprate superconductors are arisen from both the strong electron correlation and impurity-scattering effects. The theory also predicts a reverse dome-like shape of the doping dependence of the microwave conductivity, which is

in a striking contrast to the dome-like shape of the doping dependence of T_c , and therefore should be verified by further experiments.

ACKNOWLEDGEMENTS

This work is supported by the National Key Research and Development Program of China under Grant

No. 2021YFA1401803, and the National Natural Science Foundation of China under Grant Nos. 12247116, 11974051, and 12274036.

Appendix A: Derivation of vertex kernels of electron current-current correlation function

Starting from the homogenous part of the d-wave BCS type formalism, the electron current-current correlation function has been discussed by taking into account the impurity-induced vertex correction^{26–32}, where the T -matrix approach has been employed to derive the vertex kernels of the electron current-current correlation function in the nodal approximation. In this Appendix A, we generalize these previous calculations^{26–32} for the vertex kernels of the electron current-current correlation function in the nodal approximation to the present case in the Fermi-arc-tip approximation. In the microscopic octet scattering model shown in Fig. 1, the tips of the Fermi arcs labelled by the odd numbers are located in the region A of BZ, where $|k_y| > |k_x|$, while the tips of the Fermi arcs labelled by the even numbers are located in the region B of BZ, where $|k_x| > |k_y|$. For a convenience in the following discussions, $j = 1$ in Eq. (21a) is chosen in the region A of BZ, and $j = 2$ in Eq. (21b) is chosen in the region B of BZ, then the trace of the product between the self-consistent equation (21a) and the unit vector $\hat{k}_x^{(1)}$ in the region A and the trace of the product between the self-consistent equation (21b) and the unit vector $\hat{k}_x^{(2)}$ in the region B can be obtained as,

$$\begin{aligned} Tr[\tau_0 \tilde{\Lambda}_x^{(A)}(\omega, \Omega)] &= \frac{n_i N}{\cos^2 \theta_F^{(A)}} \sum_{\mathbf{k} \in A} Tr[\tilde{G}_I^{(A)}(\mathbf{k}, \omega) \sum_{j'' \in \text{odd}} \hat{k}_x^{(1)} \cdot \hat{k}_F^{(j'')} \tilde{T}_{j''1}(\omega) \tilde{T}_{1j''}(\omega + \Omega) \tilde{G}_I^{(A)}(\mathbf{k}, \omega + \Omega) [\tau_0 + \tilde{\Lambda}_x^{(A)}(\omega, \Omega)]] \\ &+ \frac{n_i N}{\cos^2 \theta_F^{(A)}} \sum_{\mathbf{k} \in B} Tr[\tilde{G}_I^{(B)}(\mathbf{k}, \omega) \sum_{j'' \in \text{even}} \hat{k}_x^{(1)} \cdot \hat{k}_F^{(j'')} \tilde{T}_{j''1}(\omega) \tilde{T}_{1j''}(\omega + \Omega) \tilde{G}_I^{(B)}(\mathbf{k}, \omega + \Omega) [\tau_0 + \tilde{\Lambda}_x^{(B)}(\omega, \Omega)]], \end{aligned} \quad (\text{A1a})$$

$$\begin{aligned} Tr[\tau_0 \tilde{\Lambda}_x^{(B)}(\omega, \Omega)] &= \frac{n_i N}{\cos^2 \theta_F^{(B)}} \sum_{\mathbf{k} \in A} Tr[\tilde{G}_I^{(A)}(\mathbf{k}, \omega) \sum_{j'' \in \text{odd}} \hat{k}_x^{(2)} \cdot \hat{k}_F^{(j'')} \tilde{T}_{j''2}(\omega) \tilde{T}_{2j''}(\omega + \Omega) \tilde{G}_I^{(A)}(\mathbf{k}, \omega + \Omega) [\tau_0 + \tilde{\Lambda}_x^{(A)}(\omega, \Omega)]] \\ &+ \frac{n_i N}{\cos^2 \theta_F^{(B)}} \sum_{\mathbf{k} \in B} Tr[\tilde{G}_I^{(B)}(\mathbf{k}, \omega) \sum_{j'' \in \text{even}} \hat{k}_x^{(2)} \cdot \hat{k}_F^{(j'')} \tilde{T}_{j''2}(\omega) \tilde{T}_{2j''}(\omega + \Omega) \tilde{G}_I^{(B)}(\mathbf{k}, \omega + \Omega) [\tau_0 + \tilde{\Lambda}_x^{(B)}(\omega, \Omega)]], \end{aligned} \quad (\text{A1b})$$

respectively, where the Fermi velocity unit vectors $\hat{k}_F^{(j)}$ with $j = 1, 2, 3, \dots, 8$ at the tips of the Fermi-arc are defined as follows: $\hat{k}_F^{(1)} = \hat{k}_x \cos \theta_F + \hat{k}_y \sin \theta_F$, $\hat{k}_F^{(2)} = \hat{k}_x \sin \theta_F + \hat{k}_y \cos \theta_F$, $\hat{k}_F^{(3)} = \hat{k}_x \cos \theta_F - \hat{k}_y \sin \theta_F$, $\hat{k}_F^{(4)} = \hat{k}_x \sin \theta_F - \hat{k}_y \cos \theta_F$, $\hat{k}_F^{(5)} = -\hat{k}_x \cos \theta_F - \hat{k}_y \sin \theta_F$, $\hat{k}_F^{(6)} = -\hat{k}_x \sin \theta_F - \hat{k}_y \cos \theta_F$, $\hat{k}_F^{(7)} = -\hat{k}_x \cos \theta_F + \hat{k}_y \sin \theta_F$, $\hat{k}_F^{(8)} = -\hat{k}_x \sin \theta_F + \hat{k}_y \cos \theta_F$. In particular, it is easy to verify the following relations,

$$\begin{aligned} \frac{n_i N}{\cos^2 \theta_F} \sum_{j'' \in \text{odd}} \hat{k}_x^{(1)} \cdot \hat{k}_F^{(j'')} \tilde{T}_{j''1}(\omega) \tilde{T}_{1j''}(\omega + \Omega) &= n_i N \left[\tilde{T}_{11}(\omega) \tilde{T}_{11}(\omega + \Omega) + \tilde{T}_{31}(\omega) \tilde{T}_{13}(\omega + \Omega) \right. \\ &\quad \left. - \tilde{T}_{51}(\omega) \tilde{T}_{15}(\omega + \Omega) - \tilde{T}_{71}(\omega) \tilde{T}_{17}(\omega + \Omega) \right], \end{aligned} \quad (\text{A2a})$$

$$\begin{aligned} \frac{n_i N}{\cos^2 \theta_F} \sum_{j'' \in \text{even}} \hat{k}_x^{(1)} \cdot \hat{k}_F^{(j'')} \tilde{T}_{j''1}(\omega) \tilde{T}_{1j''}(\omega + \Omega) &= \tan \theta_F n_i N \left[\tilde{T}_{21}(\omega) \tilde{T}_{12}(\omega + \Omega) + \tilde{T}_{41}(\omega) \tilde{T}_{14}(\omega + \Omega) \right. \\ &\quad \left. - \tilde{T}_{61}(\omega) \tilde{T}_{16}(\omega + \Omega) - \tilde{T}_{81}(\omega) \tilde{T}_{18}(\omega + \Omega) \right], \end{aligned} \quad (\text{A2b})$$

$$\begin{aligned} \frac{n_i N}{\sin^2 \theta_F} \sum_{j'' \in \text{odd}} \hat{k}_x^{(2)} \cdot \hat{k}_F^{(j'')} \tilde{T}_{j''2}(\omega) \tilde{T}_{2j''}(\omega + \Omega) &= \cot \theta_F n_i N \left[\tilde{T}_{12}(\omega) \tilde{T}_{21}(\omega + \Omega) + \tilde{T}_{32}(\omega) \tilde{T}_{23}(\omega + \Omega) \right. \\ &\quad \left. - \tilde{T}_{52}(\omega) \tilde{T}_{25}(\omega + \Omega) - \tilde{T}_{72}(\omega) \tilde{T}_{27}(\omega + \Omega) \right], \end{aligned} \quad (\text{A2c})$$

$$\begin{aligned} \frac{n_i N}{\sin^2 \theta_F} \sum_{j'' \in \text{even}} \hat{k}_x^{(2)} \cdot \hat{k}_F^{(j'')} \tilde{T}_{j''2}(\omega) \tilde{T}_{2j''}(\omega + \Omega) &= n_i N \left[\tilde{T}_{22}(\omega) \tilde{T}_{22}(\omega + \Omega) + \tilde{T}_{42}(\omega) \tilde{T}_{24}(\omega + \Omega) \right. \\ &\quad \left. - \tilde{T}_{62}(\omega) \tilde{T}_{26}(\omega + \Omega) - \tilde{T}_{82}(\omega) \tilde{T}_{28}(\omega + \Omega) \right], \end{aligned} \quad (\text{A2d})$$

in the regions A and B of BZ, respectively, with the T-matrix,

$$T^{(\alpha)}(\omega) = \begin{pmatrix} T_{AA}^{(\alpha)}(\omega) & T_{AB}^{(\alpha)}(\omega) \\ T_{BA}^{(\alpha)}(\omega) & T_{BB}^{(\alpha)}(\omega) \end{pmatrix}, \quad (\text{A3})$$

where the matrixes $T_{\mu\nu}^{(\alpha)}(\omega)$ ($\mu, \nu = A, B$) with the corresponding matrix elements have been given explicitly in Ref. 49. Moreover, a general formalism is satisfied by $\tilde{T}_{jn}(\omega) \tilde{T}_{nj}(\omega + \Omega)$ as,

$$\tilde{T}_{jn}(\omega) \tilde{T}_{nj}(\omega + \Omega) = \sum_{\alpha, \beta=0}^3 \tau_\alpha T_{jn}^{(\alpha)}(\omega) \tau_\beta T_{nj}^{(\beta)}(\omega + \Omega) = \sum_{\alpha, \beta, \gamma=0}^3 i\bar{\epsilon}_{\alpha\beta\gamma} T_{jn}^{(\alpha)}(\omega) T_{nj}^{(\beta)}(\omega + \Omega) \tau_\gamma, \quad (\text{A4})$$

with $i\bar{\epsilon}_{\alpha\beta\gamma}$ that is defined as,

$$i\bar{\epsilon}_{\alpha\beta\gamma} = \delta_{\alpha\beta} \delta_{\gamma 0} + (1 - \delta_{\alpha 0}) \delta_{\beta 0} \delta_{\gamma \alpha} + \delta_{\alpha 0} (1 - \delta_{\beta 0}) \delta_{\gamma \beta} + i\epsilon_{\alpha\beta\gamma}, \quad (\text{A5})$$

where $\epsilon_{\alpha\beta\gamma}$ is the Levi-Civita tensor, and then $i\bar{\epsilon}_{\alpha\beta\gamma}$ satisfies the following identities: $\tau_\alpha \tau_\beta = \sum_\gamma i\bar{\epsilon}_{\alpha\beta\gamma} \tau_\gamma$ and $i\bar{\epsilon}_{\alpha\beta\gamma} = i\bar{\epsilon}_{\gamma\alpha\beta}$. With the help of the above general formalism (A4), the relations in Eq. (A2) can be derived as,

$$\frac{n_i N}{\cos^2 \theta_F} \sum_{j'' \in \text{odd}} \hat{k}_x^{(1)} \cdot \hat{k}_F^{(j'')} \tilde{T}_{j''1}(\omega) \tilde{T}_{1j''}(\omega + \Omega) = \sum_\gamma C_{A1}^{(x)}(\gamma) \tau_\gamma, \quad (\text{A6a})$$

$$\begin{aligned} C_{A1}^{(x)}(\gamma) &= n_i N \sum_{\alpha, \beta=0}^3 i\bar{\epsilon}_{\alpha\beta\gamma} [T_{11}^{(\alpha)}(\omega) T_{11}^{(\beta)}(\omega + \Omega) + T_{31}^{(\alpha)}(\omega) T_{13}^{(\beta)}(\omega + \Omega) - T_{51}^{(\alpha)}(\omega) T_{15}^{(\beta)}(\omega + \Omega) \\ &\quad - T_{71}^{(\alpha)}(\omega) T_{17}^{(\beta)}(\omega + \Omega)], \end{aligned} \quad (\text{A6b})$$

$$\frac{n_i N}{\sin^2 \theta_F} \sum_{j'' \in \text{odd}} \hat{k}_x^{(2)} \cdot \hat{k}_F^{(j'')} \tilde{T}_{j''1}(\omega) \tilde{T}_{1j''}(\omega + \Omega) = \sum_\gamma C_{A2}^{(x)}(\gamma) \tau_\gamma, \quad (\text{A6c})$$

$$\begin{aligned} C_{A2}^{(x)}(\gamma) &= \cot \theta_F n_i N \sum_{\alpha, \beta=0}^3 i\bar{\epsilon}_{\alpha\beta\gamma} [T_{12}^{(\alpha)}(\omega) T_{21}^{(\beta)}(\omega + \Omega) + T_{32}^{(\alpha)}(\omega) T_{23}^{(\beta)}(\omega + \Omega) - T_{52}^{(\alpha)}(\omega) T_{25}^{(\beta)}(\omega + \Omega) \\ &\quad - T_{72}^{(\alpha)}(\omega) T_{27}^{(\beta)}(\omega + \Omega)], \end{aligned} \quad (\text{A6d})$$

$$\frac{n_i N}{\cos^2 \theta_F} \sum_{j'' \in \text{even}} \hat{k}_x^{(1)} \cdot \hat{k}_F^{(j'')} \tilde{T}_{j''1}(\omega) \tilde{T}_{1j''}(\omega + \Omega) = \sum_\gamma C_{B1}^{(x)}(\gamma) \tau_\gamma, \quad (\text{A6e})$$

$$\begin{aligned} C_{B1}^{(x)}(\gamma) &= n_i N \tan \theta_F \sum_{\alpha, \beta=0}^3 i\bar{\epsilon}_{\alpha\beta\gamma} [T_{21}^{(\alpha)}(\omega) T_{12}^{(\beta)}(\omega + \Omega) + T_{41}^{(\alpha)}(\omega) T_{14}^{(\beta)}(\omega + \Omega) - T_{61}^{(\alpha)}(\omega) T_{16}^{(\beta)}(\omega + \Omega) \\ &\quad - T_{81}^{(\alpha)}(\omega) T_{18}^{(\beta)}(\omega + \Omega)], \end{aligned} \quad (\text{A6f})$$

$$\frac{n_i N}{\sin^2 \theta_F} \sum_{j'' \in \text{even}} \hat{k}_x^{(2)} \cdot \hat{k}_F^{(j'')} \tilde{T}_{j''2}(\omega) \tilde{T}_{2j''}(\omega + \Omega) = \sum_\gamma C_{B2}^{(x)}(\gamma) \tau_\gamma, \quad (\text{A6g})$$

$$\begin{aligned} C_{B2}^{(x)}(\gamma) &= n_i N \sum_{\alpha, \beta=0}^3 i\bar{\epsilon}_{\alpha\beta\gamma} [T_{22}^{(\alpha)}(\omega) T_{22}^{(\beta)}(\omega + \Omega) + T_{42}^{(\alpha)}(\omega) T_{24}^{(\beta)}(\omega + \Omega) - T_{62}^{(\alpha)}(\omega) T_{26}^{(\beta)}(\omega + \Omega) \\ &\quad - T_{82}^{(\alpha)}(\omega) T_{28}^{(\beta)}(\omega + \Omega)]. \end{aligned} \quad (\text{A6h})$$

Substituting the above results in Eq. (A6) into Eq. (A1a) and Eq. (A1b), $Tr[\tau_0 \tilde{\Lambda}_x^{(A)}(\omega, \Omega)]$ and $Tr[\tau_0 \tilde{\Lambda}_x^{(B)}(\omega, \Omega)]$

can be obtained explicitly as,

$$Tr[\tilde{\Lambda}_x^{(A)}(\omega, \Omega)] = \sum_{\beta=0}^3 \left\{ Tr[\tau_\beta[\tau_0 + \tilde{\Lambda}_x^{(A)}(\omega, \Omega)]] R_{A1\beta}^{(x)}(\omega, \omega + \Omega) + Tr[\tau_\beta[\tau_0 + \tilde{\Lambda}_x^{(B)}(\omega, \Omega)]] R_{B1\beta}^{(x)}(\omega, \omega + \Omega) \right\}, \quad (A7a)$$

$$Tr[\tilde{\Lambda}_x^{(B)}(\omega, \Omega)] = \sum_{\beta=0}^3 \left\{ Tr[\tau_\beta[\tau_0 + \tilde{\Lambda}_x^{(A)}(\omega, \Omega)]] R_{A2\beta}^{(x)}(\omega, \omega + \Omega) + Tr[\tau_\beta[\tau_0 + \tilde{\Lambda}_x^{(B)}(\omega, \Omega)]] R_{B2\beta}^{(x)}(\omega, \omega + \Omega) \right\}, \quad (A7b)$$

respectively, with the functions,

$$R_{A1\beta}^{(x)}(\omega, \omega + \Omega) = \sum_{\gamma=0}^3 C_{A1}^{(x)}(\gamma) \tilde{I}_\gamma^{(A)}(\beta, \omega, \omega + \Omega), \quad R_{A2\beta}^{(x)}(\omega, \omega + \Omega) = \sum_{\gamma=0}^3 C_{A2}^{(x)}(\gamma) \tilde{I}_\gamma^{(A)}(\beta, \omega, \omega + \Omega), \quad (A8a)$$

$$R_{B1\beta}^{(x)}(\omega, \omega + \Omega) = \sum_{\gamma=0}^3 C_{B1}^{(x)}(\gamma) \tilde{I}_\gamma^{(B)}(\beta, \omega, \omega + \Omega), \quad R_{B2\beta}^{(x)}(\omega, \omega + \Omega) = \sum_{\gamma=0}^3 C_{B2}^{(x)}(\gamma) \tilde{I}_\gamma^{(B)}(\beta, \omega, \omega + \Omega). \quad (A8b)$$

Now we turn to evaluate the similar traces of the product between the vertex kernel $\tilde{\Lambda}_x^{(A)}(\omega, \Omega)$ and matrix τ_α with $\alpha = 1, 2, 3$ in the region A and the product of the vertex kernel $\tilde{\Lambda}_x^{(B)}(\omega, \Omega)$ and matrix τ_α in the region B in the kernel function (25), where the derivation processes are almost the same as the derivation processes for the above $Tr[\tau_0 \tilde{\Lambda}_x^{(A)}(\omega, \Omega)]$ in Eq. (A7a) and $Tr[\tau_0 \tilde{\Lambda}_x^{(B)}(\omega, \Omega)]$ in Eq. (A7b), and the obtained results can be expressed explicitly as,

$$Tr[\tau_\alpha \tilde{\Lambda}_x^{(A)}(\omega, \Omega)] = \sum_{\beta=0}^3 \left\{ Tr[\tau_\beta[\tau_0 + \tilde{\Lambda}_x^{(A)}(\omega, \Omega)]] R_{A1\beta}^{(x)}(\alpha, \omega, \omega + \Omega) + Tr[\tau_\beta[\tau_0 + \tilde{\Lambda}_x^{(B)}(\omega, \Omega)]] R_{B1\beta}^{(x)}(\alpha, \omega, \omega + \Omega) \right\}, \quad (A9a)$$

$$Tr[\tau_\alpha \tilde{\Lambda}_x^{(B)}(\omega, \Omega)] = \sum_{\beta=0}^3 \left\{ Tr[\tau_\beta[\tau_0 + \tilde{\Lambda}_x^{(A)}(\omega, \Omega)]] R_{A2\beta}^{(x)}(\alpha, \omega, \omega + \Omega) + Tr[\tau_\beta[\tau_0 + \tilde{\Lambda}_x^{(B)}(\omega, \Omega)]] R_{B2\beta}^{(x)}(\alpha, \omega, \omega + \Omega) \right\}, \quad (A9b)$$

with the functions,

$$R_{A1\beta}^{(x)}(\alpha, \omega, \omega + \Omega) = \sum_{\lambda=0}^3 C_{A1\alpha}^{(x)}(\lambda) \tilde{I}_\lambda^{(A)}(\beta, \omega, \omega + \Omega), \quad (A10a)$$

$$C_{A1\alpha}^{(x)}(\lambda) = n_i N \sum_{\mu, \nu=0}^3 \left(\sum_{\sigma} i \bar{\epsilon}_{\mu\nu\sigma} i \bar{\epsilon}_{\sigma\alpha\lambda} \right) \eta_\alpha(\nu) [T_{11}^{(\mu)}(\omega) T_{11}^{(\nu)}(\omega + \Omega) + T_{31}^{(\mu)}(\omega) T_{13}^{(\nu)}(\omega + \Omega) - T_{51}^{(\mu)}(\omega) T_{15}^{(\nu)}(\omega + \Omega) - T_{71}^{(\mu)}(\omega) T_{17}^{(\nu)}(\omega + \Omega)], \quad (A10b)$$

$$R_{B1\beta}^{(x)}(\alpha, \omega, \omega + \Omega) = \sum_{\lambda=0}^3 C_{B1\alpha}^{(x)}(\lambda) \tilde{I}_\lambda^{(B)}(\beta, \omega, \omega + \Omega), \quad (A10c)$$

$$C_{B1\alpha}^{(x)}(\lambda) = n_i N \tan \theta_F \sum_{\mu, \nu=0}^3 \left(\sum_{\sigma} i \bar{\epsilon}_{\mu\nu\sigma} i \bar{\epsilon}_{\sigma\alpha\lambda} \right) \eta_\alpha(\nu) [T_{21}^{(\mu)}(\omega) T_{12}^{(\nu)}(\omega + \Omega) + T_{41}^{(\mu)}(\omega) T_{14}^{(\nu)}(\omega + \Omega) - T_{61}^{(\mu)}(\omega) T_{16}^{(\nu)}(\omega + \Omega) - T_{81}^{(\mu)}(\omega) T_{18}^{(\nu)}(\omega + \Omega)], \quad (A10d)$$

$$R_{A2\beta}^{(x)}(\alpha, \omega, \omega + \Omega) = \sum_{\lambda=0}^3 C_{A2\alpha}^{(x)}(\lambda) \tilde{I}_\lambda^{(A)}(\beta, \omega, \omega + \Omega), \quad (A10e)$$

$$C_{A2\alpha}^{(x)}(\lambda) = n_i N \cot \theta_F \sum_{\mu, \nu=0}^3 \left(\sum_{\sigma} i \bar{\epsilon}_{\mu\nu\sigma} i \bar{\epsilon}_{\sigma\alpha\lambda} \right) \eta_\alpha(\nu) [T_{12}^{(\mu)}(\omega) T_{21}^{(\nu)}(\omega + \Omega) + T_{32}^{(\mu)}(\omega) T_{23}^{(\nu)}(\omega + \Omega) - T_{52}^{(\mu)}(\omega) T_{25}^{(\nu)}(\omega + \Omega) - T_{72}^{(\mu)}(\omega) T_{27}^{(\nu)}(\omega + \Omega)], \quad (A10f)$$

$$R_{B2\beta}^{(x)}(\alpha, \omega, \omega + \Omega) = \sum_{\lambda=0}^3 C_{B2\alpha}^{(x)}(\lambda) \tilde{I}_\lambda^{(B)}(\beta, \omega, \omega + \Omega), \quad (A10g)$$

$$\begin{aligned}
C_{B2\alpha}^{(x)}(\lambda) &= n_i N \sum_{\mu, \nu=0}^3 \left(\sum_{\sigma} i\bar{\epsilon}_{\mu\nu\sigma} i\bar{\epsilon}_{\sigma\alpha\lambda} \right) \eta_{\alpha}(\nu) [T_{22}^{(\mu)}(\omega) T_{22}^{(\nu)}(\omega + \Omega) + T_{42}^{(\mu)}(\omega) T_{24}^{(\nu)}(\omega + \Omega) \\
&\quad - T_{62}^{(\mu)}(\omega) T_{26}^{(\nu)}(\omega + \Omega) - T_{82}^{(\mu)}(\omega) T_{28}^{(\nu)}(\omega + \Omega)],
\end{aligned} \tag{A10h}$$

where $\sum_{\sigma} i\bar{\epsilon}_{\mu\nu\sigma} i\bar{\epsilon}_{\sigma\alpha\lambda}$ satisfies the following identity,

$$\begin{aligned}
\sum_{\sigma} i\bar{\epsilon}_{\mu\nu\sigma} i\bar{\epsilon}_{\sigma\alpha\lambda} &= -4\delta_{\mu 0}\delta_{\nu 0}\delta_{\alpha 0}\delta_{\lambda 0} + \delta_{\alpha\mu}\delta_{\lambda 0}\delta_{\nu 0} + \delta_{\alpha\nu}\delta_{\mu 0}\delta_{\lambda 0} + \delta_{\lambda\mu}\delta_{\nu 0}\delta_{\alpha 0} + \delta_{\mu 0}\delta_{\alpha 0}\delta_{\lambda\nu} + \delta_{\alpha\lambda}\delta_{\mu\nu} + \delta_{\alpha\nu}\delta_{\lambda\mu} - \delta_{\alpha\mu}\delta_{\lambda\nu} \\
&\quad + i\delta_{\alpha 0}\epsilon_{\lambda\mu\nu} + i\delta_{\lambda 0}\epsilon_{\alpha\mu\nu} + i\delta_{\mu 0}\epsilon_{\nu\alpha\lambda} + i\delta_{\nu 0}\epsilon_{\mu\alpha\lambda},
\end{aligned} \tag{A11}$$

and the tensor $\eta_{\alpha}(\nu)$ is defined as,

$$\eta_{\alpha}(\nu) = \begin{cases} 1, & \nu = 0, \alpha \\ -1, & \text{others.} \end{cases} \tag{A12}$$

Substituting the above results in Eqs. (A7) and (A9) into Eq. (25) of the main text, we therefore obtain the kernel function $J_{xx}(\omega, \omega + \Omega)$ in Eq. (25) of the main text.

* spfeng@bnu.edu.cn

- ¹ J. R. Schrieffer, *Theory of Superconductivity*, (Benjamin, New York, 1964).
- ² P. W. Anderson, Phys. Rev. **109**, 1492 (1958).
- ³ D. N. Basov, and T. Timusk, in *Handbook on the Physics and Chemistry of Rare Earths*, Vol. 31 (Elsevier Science, Amsterdam, 2001), p. 437.
- ⁴ See, e.g., the review, N. E. Hussey, Adv. Phys. **51**, 1685 (2002).
- ⁵ See, e.g., the review, A. V. Balatsky, I. Vekhter, and J.-X. Zhu, Rev. Mod. Phys. **78**, 373 (2006).
- ⁶ See, e.g., the review, H. Alloul, J. Bobroff, M. Gabay, and P. J. Hirschfeld, Rev. Mod. Phys. **81**, 45 (2009).
- ⁷ See e.g., the review, C. C. Tsuei and J. R. Kirtley, Rev. Mod. Phys. **72**, 969 (2000).
- ⁸ K. Ishida, Y. Kitaoka, T. Yoshitomi, N. Ogata, T. Kamino, and K. Asayama, Physica C **179**, 29 (1991).
- ⁹ A. Legris, F. Rullier-Albenque, E. Radeva, and P. Lejay, J. Phys. I **3**, 1605 (1993).
- ¹⁰ J. Giapintzakis, D. M. Ginsberg, M. A. Kirk, and S. Ockers, Phys. Rev. B **50**, 15967 (1994).
- ¹¹ Y. Fukuzumi, K. Mizuhashi, K. Takenaka, and S. Uchida, Phys. Rev. Lett. **76**, 684 (1996).
- ¹² S. K. Tolpygo, J.-Y. Lin, M. Gurrutxaga, S. Y. Hou, and J. M. Phillips, Phys. Rev. B **53**, 12454 (1996).
- ¹³ J. P. Attfield, A. L. Kharlanov, and J. A. McAllister, Nature **394**, 157 (1998).
- ¹⁴ J. Bobroff, W. A. MacFarlane, H. Alloul, P. Mendels, N. Blanchard, G. Collin, and J.-F. Marucco, Phys. Rev. Lett. **83**, 4381 (1999).
- ¹⁵ H. Eisaki, N. Kaneko, D. L. Feng, A. Damascelli, P. K. Mang, K. M. Shen, Z.-X. Shen, and M. Greven, Phys. Rev. B **69**, 064512 (2004).
- ¹⁶ D. A. Bonn, R. Liang, T. M. Riseman, D. J. Baar, D. C. Morgan, K. Zhang, P. Dosanjh, T. L. Duty, A. MacFarlane, G. D. Morris, J. H. Brewer, W. N. Hardy, C. Kallin, and A. J. Berlinsky, Phys. Rev. B **47**, 11314 (1993).
- ¹⁷ S.-F. Lee, D. C. Morgan, R. J. Ormeno, D. M. Broun, R. A. Doyle, J. R. Waldram, and K. Kadowaki, Phys. Rev. Lett. **77**, 735 (1996).
- ¹⁸ A. Hosseini, R. Harris, S. Kamal, P. Dosanjh, J. Preston, R. Liang, W. N. Hardy, and D. A. Bonn, Phys. Rev. B **60**, 1349 (1999).
- ¹⁹ P. J. Turner, R. Harris, S. Kamal, M. E. Hayden, D. M. Broun, D. C. Morgan, A. Hosseini, P. Dosanjh, G. K. Mullins, J. S. Preston, R. Liang, D. A. Bonn, and W. N. Hardy, Phys. Rev. Lett. **90**, 237005 (2003).
- ²⁰ R. Harris, P. J. Turner, S. Kamal, A. R. Hosseini, P. Dosanjh, G. K. Mullins, J. S. Bobowski, C. P. Bidinosti, D. M. Broun, R. Liang, W. N. Hardy, and D. A. Bonn, Phys. Rev. B **74**, 104508 (2006).
- ²¹ D. A. Bonn, S. Kamal, K. Zhang, R. Liang, D. J. Baar, E. Klein, and W. N. Hardy, Phys. Rev. B **50**, 4051 (1994).
- ²² C. Bucci, P. Carretta, R. D. Renzi, G. Guidia, F. Licci, L. G. Raftob, H. Keller, S. Lee, I. M. Savić, Physica C **235-240**, 1849 (1994).
- ²³ C. Bernhard, J. L. Tallon, C. Bucci, R. DeRenzi, G. Guidi, G. V. M. Williams, and C. Niedermayer, Phys. Rev. Lett. **77**, 2304 (1996).
- ²⁴ J. Bobroff, Ann. Phys. (Paris) **30**, 1 (2005).
- ²⁵ P. J. Hirschfeld, W. O. Putikka, and D. J. Scalapino, Phys. Rev. B **50**, 10250 (1994).
- ²⁶ A. C. Durst and P. A. Lee, Phys. Rev. B **62**, 1270 (2000).
- ²⁷ A. J. Berlinsky, D. A. Bonn, R. Harris, and C. Kallin, Phys. Rev. B **61**, 9088 (2000).
- ²⁸ M. H. Hettler and P. J. Hirschfeld, Phys. Rev. B **61**, 11313 (2000).
- ²⁹ A. C. Durst and P. A. Lee, Phys. Rev. B **65**, 094501 (2002).
- ³⁰ W. Kim, F. Marsiglio, and J. P. Carbotte, Phys. Rev. B **70**, 060505(R) (2004).
- ³¹ T. S. Nunner and P. J. Hirschfeld, Phys. Rev. B **72**, 014514 (2005).
- ³² Z. Wang, H. Guo, and S. Feng, Physica C **468**, 1078 (2008); Z. Wang and S. Feng, Phys. Rev. B **80**, 174507 (2009).

- ³³ U. Chatterjee, M. Shi, A. Kaminski, A. Kanigel, H. M. Fretwell, K. Terashima, T. Takahashi, S. Rosenkranz, Z. Z. Li, H. Raffy, A. Santander-Syro, K. Kadowaki, M. R. Norman, M. Randeria, and J. C. Campuzano, *Phys. Rev. Lett.* **96**, 107006 (2006).
- ³⁴ Y. He, Y. Yin, M. Zech, A. Soumyanarayanan, M. M. Yee, T. Williams, M. C. Boyer, K. Chatterjee, W. D. Wise, I. Zeljkovic, T. Kondo, T. Takeuchi, H. Ikuta, P. Mistark, R. S. Markiewicz, A. Bansil, S. Sachdev, E. W. Hudson, and J. E. Hoffman, *Science* **344**, 608 (2014).
- ³⁵ F. Restrepo, J. Zhao, J. C. Campuzano, and U. Chatterjee, *Phys. Rev. B* **107**, 174519 (2023).
- ³⁶ M. R. Norman, H. Ding, M. Randeria, J. C. Campuzano, T. Yokoya, T. Takeuchi, T. Takahashi, T. Mochiku, K. Kadowaki, P. Guptasarma, and D. G. Hinks, *Nature* **392**, 157 (1998).
- ³⁷ M. Shi, J. Chang, S. Pailh es, M. R. Norman, J. C. Campuzano, M. M ansson, T. Claesson, O. Tjernberg, A. Bendounan, L. Patthey, N. Momono, M. Oda, M. Ido, C. Mudry, and J. Mesot, *Phys. Rev. Lett.* **101**, 047002 (2008).
- ³⁸ Y. Sassa, M. Radovi c, M. M ansson, E. Razzoli, X. Y. Cui, S. Pailh es, S. Guerrero, M. Shi, P. R. Willmott, F. Miletto Granozio, J. Mesot, M. R. Norman, and L. Patthey, *Phys. Rev. B* **83**, 140511(R) (2011).
- ³⁹ K. Fujita, C. K. Kim, I. Lee, J. Lee, M. H. Hamidian, I. A. Firmo, S. Mukhopadhyay, H. Eisaki, S. Uchida, M. J. Lawler, E.-A. Kim, and J. C. Davis, *Science* **344**, 612 (2014).
- ⁴⁰ R. Comin, A. Frano, M. M. Yee, Y. Yoshida, H. Eisaki, E. Schierle, E. Weschke, R. Sutarto, F. He, A. Soumyanarayanan, Yang He, M. L. Tacon, I. S. Elfimov, Jennifer E. Hoffman, G. A. Sawatzky, B. Keimer, and A. Damascelli, *Science* **343**, 390 (2014).
- ⁴¹ A. Kaminski, T. Kondo, T. Takeuchi, and G. Gu, *Phil. Mag.* **95**, 453 (2015).
- ⁴² B. Loret, S. Sakai, S. Benhabib, Y. Gallais, M. Cazayous, M. A. M easson, R. D. Zhong, J. Schneeloch, G. D. Gu, A. Forget, D. Colson, I. Paul, M. Civelli, and A. Sacuto, *Phys. Rev. B* **96**, 094525 (2017).
- ⁴³ S. D. Chen, M. Hashimoto, Y. He, D. Song, K. J. Xu, J. F. He, T. P. Devereaux, H. Eisaki, D. H. Lu, J. Zaanen, and Z. -X. Shen, *Science* **366**, 1099 (2019).
- ⁴⁴ See, e.g., the review, J.-X. Yin, S. H. Pan, and M. Z. Hasan, *Nat. Rev. Phys.* **3**, 249 (2021).
- ⁴⁵ S. H. Pan, J. P.  Neal, R. L. Badzey, C. Chamon, H. Ding, J. R. Engelbrecht, Z. Wang, H. Eisaki, S. Uchida, A. K. Gupta, K.-W. Ng, E. W. Hudson, K. M. Lang, and J. C. Davis, *Nature* **413**, 282 (2001).
- ⁴⁶ Y. Kohsaka, C. Taylor, K. Fujita, A. Schmidt, C. Lupien, T. Hanaguri, M. Azuma, M. Takano, H. Eisaki, H. Takagi, S. Uchida, and J. C. Davis, *Science* **315**, 1380 (2007).
- ⁴⁷ Y. Kohsaka, C. Taylor, P. Wahl, A. Schmidt, J. Lee, K. Fujita, J. W. Alldredge, K. McElroy, J. Lee, H. Eisaki, S. Uchida, D.-H. Lee, and J. C. Davis, *Nature* **454**, 1072 (2008).
- ⁴⁸ M. H. Hamidian, S. D. Edkins, S. Hyun Joo, A. Kostin, H. Eisaki, S. Uchida, M. J. Lawler, E.-A. Kim, A. P. Mackenzie, K. Fujita, J. Lee, and J. C. S. Davis, *Nature* **532**, 343 (2016).
- ⁴⁹ M. Zeng, X. Li, Y. Wang, and S. Feng, *Phys. Rev. B* **106**, 054512 (2022).
- ⁵⁰ S. Feng, *Phys. Rev. B* **68**, 184501 (2003); S. Feng, T. Ma, and H. Guo, *Physica C* **436**, 14 (2006).
- ⁵¹ S. Feng, H. Zhao, and Z. Huang, *Phys. Rev. B* **85**, 054509 (2012); *Phys. Rev. B* **85**, 099902(E) (2012).
- ⁵² See, e.g., the review, S. Feng, Y. Lan, H. Zhao, L. Kuang, L. Qin, and X. Ma, *Int. J. Mod. Phys. B* **29**, 1530009 (2015).
- ⁵³ S. Feng, L. Kuang, and H. Zhao, *Physica C* **517**, 5 (2015).
- ⁵⁴ P. W. Anderson, *Science* **235**, 1196 (1987).
- ⁵⁵ F. C. Zhang and T. M. Rice, *Phys. Rev. B* **37**, 3759 (1988).
- ⁵⁶ See, e.g., the review, L. Yu, in *Recent Progress in Many-Body Theories*, edited by T. L. Ainsworth, C. E. Campbell, B. E. Clements, and E. Krotscheck (Plenum, New York, 1992), Vol. **3**, p. 157.
- ⁵⁷ S. Feng, J. B. Wu, Z. B. Su, and L. Yu, *Phys. Rev. B* **47**, 15192 (1993).
- ⁵⁸ L. Zhang, J. K. Jain, and V. J. Emery, *Phys. Rev. B* **47**, 3368 (1993).
- ⁵⁹ J. C. LeGuillou and E. Ragoucy, *Phys. Rev. B* **52**, 2403 (1995).
- ⁶⁰ S. Feng, J. Qin, and T. Ma, *J. Phys.: Condens. Matter* **16**, 343 (2004); S. Feng, Z. B. Su, and L. Yu, *Phys. Rev. B* **49**, 2368 (1994).
- ⁶¹ Y. Liu, Y. Lan, and S. Feng, *Phys. Rev. B* **103**, 024525 (2021).
- ⁶² D. Gao, Y. Liu, H. Zhao, Y. Mou, and S. Feng, *Physica C* **551**, 72 (2018).
- ⁶³ D. Gao, Y. Mou, Y. Liu, S. Tan, and S. Feng, *Phil. Mag.* **99**, 752 (2019).
- ⁶⁴ See, e.g., G. D. Mahan, *Many-Particle Physics*, (Plenum Press, New York, 1981).
- ⁶⁵ P. J. Hirschfeld, P. W olfle, J. A. Sauls, D. Einzel, and W. O. Putikka, *Phys. Rev. B* **40**, 6695 (1989).
- ⁶⁶ P. J. Hirschfeld and N. Goldenfeld, *Phys. Rev. B* **48**, 4219 (1993).
- ⁶⁷ D. S. Dessau, B. O. Wells, Z.-X. Shen, W. E. Spicer, A. J. Arko, R. S. List, D. B. Mitzi, and A. Kapitulnik, *Phys. Rev. Lett.* **66**, 2160 (1991).
- ⁶⁸ Y. Hwu, L. Lozzi, M. Marsi, S. LaRosa, M. Winokur, P. Davis, M. Onellion, H. Berger, F. Gozzo, F. L evy, and G. Margaritondo, *Phys. Rev. Lett.* **67**, 2573 (1991).
- ⁶⁹ M. Randeria, H. Ding, J.-C. Campuzano, A. Bellman, G. Jennings, T. Yokoya, T. Takahashi, H. Katayama-Yoshida, T. Mochiku, and K. Kadowaki, *Phys. Rev. Lett.* **74**, 4951 (1995).
- ⁷⁰ A. V. Fedorov, T. Valla, P. D. Johnson, Q. Li, G. D. Gu, and N. Koshizuka, *Phys. Rev. Lett.* **82**, 2179 (1999).
- ⁷¹ D. H. Lu, D. L. Feng, N. P. Armitage, K. M. Shen, A. Damascelli, C. Kim, F. Ronning, Z.-X. Shen, D. A. Bonn, R. Liang, W. N. Hardy, A. I. Rykov, and S. Tajima, *Phys. Rev. Lett.* **86**, 4370 (2001).
- ⁷² S. Sakai, S. Blanc, M. Civelli, Y. Gallais, M. Cazayous, M.-A. M easson, J. S. Wen, Z. J. Xu, G. D. Gu, G. Sangiovanni, Y. Motome, K. Held, A. Sacuto, A. Georges, and M. Imada, *Phys. Rev. Lett.* **111**, 107001 (2013).
- ⁷³ D. Mou, A. Kaminski, and G. Gu, *Phys. Rev. B* **95**, 174501 (2017).